

Research



**Cite this article:** Palazzo O, Rass M, Brembs B. 2020 Identification of *FoxP* circuits involved in locomotion and object fixation in *Drosophila*. *Open Biol.* **10**: 200295.  
<https://doi.org/10.1098/rsob.200295>

Received: 14 September 2020  
Accepted: 10 November 2020

**Subject Area:**

genetics/neuroscience/molecular biology

**Keywords:**

*FoxP*, *Drosophila*, behavioural biology, molecular biology

**Author for correspondence:**

Björn Brembs  
e-mail: [bjorn@brembs.net](mailto:bjorn@brembs.net)

# Identification of *FoxP* circuits involved in locomotion and object fixation in *Drosophila*

Ottavia Palazzo, Mathias Rass and Björn Brembs

Institut für Zoologie - Neurogenetik, Universität Regensburg, Regensburg, Germany

**id** OP, 0000-0002-3061-9643; MR, 0000-0001-7509-0336; BB, 0000-0001-7824-7650

The *FoxP* family of transcription factors is necessary for operant self-learning, an evolutionary conserved form of motor learning. The expression pattern, molecular function and mechanisms of action of the *Drosophila* *FoxP* orthologue remain to be elucidated. By editing the genomic locus of *FoxP* with CRISPR/Cas9, we find that the three different *FoxP* isoforms are expressed in neurons, but not in glia and that not all neurons express all isoforms. Furthermore, we detect *FoxP* expression in, e.g. the protocerebral bridge, the fan-shaped body and in motor neurons, but not in the mushroom bodies. Finally, we discover that *FoxP* expression during development, but not adulthood, is required for normal locomotion and landmark fixation in walking flies. While *FoxP* expression in the protocerebral bridge and motor neurons is involved in locomotion and landmark fixation, the *FoxP* gene can be excised from dorsal cluster neurons and mushroom-body Kenyon cells without affecting these behaviours.

## 1. Introduction

The family of *Forkhead Box* (*Fox*) genes comprises a large number of transcription factors that share the evolutionary conserved forkhead/winged-helix DNA-binding domain [1]. In mammals, the *FoxP* subfamily (*FoxP1-4*) members [2] are abundantly expressed during the development of multiple cell types, such as cardiomyocytes, neurons, lung epithelial secretory cells and T-cells [3]. In particular, *FoxP1* and *FoxP2* have generated interest because of their roles in regulating the development of cognitive processes such as speech and language acquisition [4–13].

Humans with *FOXP1* deletions present with mild mental retardation, delayed onset of walking, gross motor impairments and significant language and speech deficits [8]. Mutations in *FOXP2* cause a severe speech and language disorder characterized by deficits in language processing, verbal dyspraxia and impaired grammatical skills, without affecting other traits severely [4,5]. The function of *FoxP* genes in vocal learning appears to be evolutionary conserved as knock-outs of the zebra finch orthologue of human *FOXP2* during the critical song learning period alters the structure of the crystallized song in the adults [14]. Such vocal learning is a form of motor learning that proceeds slowly from highly variable ‘babbling’ (in humans) and ‘subsong’ (in zebra finches) towards more stereotypic language and crystallized song, respectively. This specific kind of learning has been classified as a form of operant learning [15–17]. It was recently shown that, as in humans and zebra finches, also in flies, *FoxP* is involved in such operant learning [18].

The original *forkhead* (*fkh*) gene was identified in the fruit fly *Drosophila melanogaster* [19], where mutations cause defects in head fold involution during embryogenesis, causing the characteristic ‘fork head’. In contrast to chordates with four *FoxP* family members, only one orthologue of the *FoxP* subfamily is present in flies (*dFoxP*). The *dFoxP* gene gives rise to three different

transcripts by alternative splicing [2,18,20]: *FoxP-isoform A* (*FoxP-iA*), *FoxP-isoform B* (*FoxP-iB*) and *FoxP-isoform IR* (Intron Retention; *FoxP-iIR*) (figure 1a). The currently available reports as to the expression pattern of the *FoxP* gene have been contradictory and nothing is known as to whether the different isoforms are differentially expressed in different cell types. To resolve these issues we have tagged the endogenous *FoxP* gene, analysed the isoform-specific expression patterns and compared them with the expression of a selection of cell-type-specific markers.

Flies with a mutated *FoxP* gene not only show impairments in operant learning, but also in motor coordination and performance of inborn behaviours [18,20–22]. While isoform-specific alleles did show different phenotypes as well as different degrees of severity of these impairments, it remains unknown which neurons require *FoxP* expression at what developmental stage(s) for normal locomotor behaviour. We therefore knocked out the *FoxP* gene in a spatiotemporally controlled manner and analysed spatial and temporal parameters of locomotor behaviour in the resulting mutants in Buridan's paradigm.

## 2. Material and methods

### 2.1. Fly strains

Fly stocks were maintained at 18°C (table 1). Before experimental use, flies were kept at 25°C, in a 12/12 h light/dark regime at 60% relative humidity for at least one generation. All crosses were raised at 25°C (except for the ones involving the temperature-sensitive Gal4 inhibitor Gal80<sup>ts</sup> [23,24] that were raised at 18°C) using four to six females and two to four males. For expression pattern visualizations, the *FoxP-iB-Gal4* and *FoxP-LexA* driver line, respectively, were crossed with the appropriate effector lines containing different GFP or RFP variants (table 1). For behavioural analysis involving the *UAS-t:gRNA(4xFoxP)*, this effector line was always first crossed with a *UAS-Cas9* line, and the resulting double-effector offspring with the appropriate driver line for each experiment (*ELAV-Gal4*, *D42-Gal4*, *C380-Gal4*, *cmPy-Gal4*, *ato-Gal4* and *ELAV-Gal4;Tub-Gal80<sup>ts</sup>*).

For local knock-out experiments, two genetic constructs need to be brought together for the method to work effectively. The endonuclease Cas9 needs to be present as well as the guide RNA (gRNA) to provide a target for the nuclease. Hence, the appropriate control groups express only one component of the CRISPR/Cas9 combination. One line drives expression only of the Cas9 endonuclease (i.e. *xxx-Gal4 > UAS-Cas9*, without gRNAs) and the other drives expression only of the gRNAs (i.e. *xxx-Gal4 > UAS-t:gRNA(4xFoxP)* without Cas9). In this fashion, each strain not only controls for potential insertion effects of the transgenes used, but also for potential detrimental effects of expressing the components alone, irrespective of the excision of the target gene.

For the behavioural analysis involving the *FoxP-KO* mutant and the *FoxP-iB-Gal4* driver line we crossed the lines back into *Wild-Type Berlin* genetic background for at least six generations in order to get the same genetic background as the *WTB* control.

### 2.2. In-silico sequences alignment

The transcript and protein sequences of the different *FoxP* isoforms were downloaded from <https://flybase.org> and

aligned with *Clustal Omega* for multiple sequence alignment. The protein domains were analysed with the *NCBI Conserved Domain Search* tool, and the stop codons were identified with *ExpASy Translate* tool (figure 1a).

### 2.3. Transgenics

We used CRISPR/Cas9 Homology-Directed Repair (HDR) to edit the *FoxP* locus [25] and generated t-RNA based vectors for producing multiple clustered regularly interspaced (CRISPR) gRNAs from a single transcript [26]. We created a total of two driver lines (*FoxP-iB-Gal4* and *FoxP-LexA*), one mutant line (*FoxP-KO*) and one effector line (*UAS-t:gRNA(4xFoxP)*).

#### 2.3.1. FoxP-iB-Gal4

To create an isoform-specific driver line, we inserted a Gal4 sequence into exon 8, which is specific to isoform B. Two 1 kb homology fragments were PCR-amplified (primers Hom1: fw 5'-GGGGGCGGCCCGCCGTGGAAGGTAAAATGCCCATATATG-3', rv 5'-GGGGCCGCGGCCCTCGTGTAAGGAAAGGTTTCGTACGAATCGC-3'; primers Hom2: fw 5'-GGGGGGCGCGCCACAAGTGCTTTGTACGTTATGAA-3', rv 5'-GGGGGTACCGGTCAGTATCGTTAATGATC-3') and digested with the appropriate restriction enzymes (Hom1: NotI and SacII, Hom2: AscI and KpnI) to be ligated in the pT-GEM(0) (Addgene plasmid no. 62891; RRID:Addgene\_62891) vector [27] which contained a Gal4 sequence and a 3xP3-RFP-SV40 sequence for selection of transformants. The gRNA sequences used are: sense 5'-CTTCGACGTACAAAGCACTTGTA-3', and asense 5'-AACTACACAAGTGCTTTGTACGTC-3'. They were annealed and cloned inside a pU6-gRNA (Addgene plasmid no. 53062; RRID:Addgene\_53062) vector [28], previously digested with BbsI restriction enzyme.

#### 2.3.2. FoxP-LexA

To create a driver line that reflects expression of all *FoxP* isoforms, we inserted a LexA sequence into exon 3. Two 1 kb homology fragments were PCR-amplified (primers Hom1: fw 5'-GGGGGCGGCCCGCCAGGAATGGCGGCATATGAGT-3', rv 5'-GGGGCCGCGGCCCTCTATTACGGTAAGCGGACTCCGG-3'; primers Hom2: fw 5'-GGCCGGTACCATAGCATAGGCCGACCCATC-3', rv 5'-GGCCACTAGTTCACATTCTCAACCCGCATAAAGC-3') and digested with the appropriate restriction enzymes (Hom1: NotI and SacII, Hom2: KpnI and SpeI) to be ligated in the pT-GEM(0) vector which contained a LexA sequence and a 3xP3-RFP-SV40 sequence for selection of transformants. The gRNA sequences used are: sense 5'-CTTCGGGTCGGCCTATGCTATTA-3', asense 5'-AACTAAATAGCATAGGCCGACCC-3'. They were annealed and were cloned inside a pU6-gRNA vector previously digested with BbsI restriction enzyme.

#### 2.3.3. FoxP-KO

To prevent expression of any isoform of the *FoxP* gene, we removed part of exon 1, the complete exon 2 and part of exon 3. Two 1 kb homology fragments were PCR-amplified (primers Hom1: fw 5'-GGGGCTAGCCAAAATAAGATGTGTCTGGTTTCCTTG-3', rv 5'-GGGCCGCGGGCATGGCGAACTCATCGTG-3', primers Hom2: fw 5'-GGGGACTAGTAGAGG GAAAGTTTTGCCGG-3', rv 5'-GGGGCTGCAGTATGAAGG



**Table 1.** Complete list of the fly lines used in this study.

genotype	use	RRID
<i>;;ok107-Gal4</i>	driver line	
<i>;;ato-Gal4;</i>	driver line	BDSC_6480
<i>;;cmpy-Gal4;</i>	driver line	BDSC_50422
<i>;;D42-Gal4;</i>	driver line	BDSC_8816
<i>;;FoxP-/-<sup>a</sup></i>	mutant	/
<i>;;FoxP-<i>iB</i>-Gal4<sup>a</sup></i>	driver line	/
<i>;;FoxP-LexA<sup>a</sup></i>	driver line	/
<i>;;UAS-t:grNA(4xFoxP)<sup>a</sup></i>	effector line	/
<i>;ELAV-Gal4;;</i>	driver line	
<i>;LexAop-mCD8-RFP-UAS-mCD8-GFP;;</i>	effector line	
<i>;LexAop-Stinger-GFP;;</i>	effector line	
<i>;Tdc2-Gal4;;</i>	driver line	BDSC_9313
<i>;UAS-Cas9;;</i>	effector line	
<i>;UAS-CD8-GFP;;</i>	effector line	
<i>;UAS-Stinger-GFP;;</i>	effector line	
<i>;Vas-Cas9</i>	mutant	
<i>C380-Gal4;;</i>	driver line	BDSC_80580
<i>CS-TZ</i>	wild-type strain	
<i>ELAV-Gal4;Tub-Gal80<sup>TS</sup>;;</i>	driver line	
<i>FoxP<sup>3955</sup></i>	mutant	
<i>Integrase(x);;AttP2</i>	mutant	
<i>w-;; D3/TM3, Sb</i>	balancer	
<i>white-/-</i>	mutant	
<i>WTB</i>	wild-type strain	

<sup>a</sup>The flies strains marked are the ones that we created in the present work.

GACAGATTGTGCCGG-3') and digested with the appropriate restriction enzymes (Hom1: NheI and SacII, Hom2: SpeI and PstI) to be ligated in the pHD-DsRed-attP (Addgene plasmid no. 51019; RRID:Addgene\_51019) vector which contains a 3xP3-DsRed sequence for selection of transformants. The gRNA sequences used are: gRNA1 sense 5'-CTTCGCGGATG ATAGTACTTCCGCA-3', asense 5'-AAACTGCGGAAGTACT ATCATCCGC-3'; gRNA2 sense 5'-CTTCGAAGGACGTGCCC GGAAGAGA-3', asense 5'-AAACTCTTCCGGCAGGTC CTTC-3'. They were annealed and were cloned inside a pU6-gRNA vector previously digested with BbsI restriction enzyme.

### 2.3.4. UAS-t:grNA(4xFoxP)

To create an isoform-unspecific conditional effector line we phosphorylated and annealed three sets of oligos (1. fw 5'-CGGCCCGGGTTTCGATTCCCGGCCGATGCAGAGCATCGA TGAATCCTCAAGTTTCAGAGCTATGCTGGAAAC-3', rv 5'-GCTCGGATATGAACTCGGGCTGCACCAGCCGGGAATCG AAC-3'; 2. fw 5'-GCCCGAGTTCATATCCGAGCGTTTCA GAGCTATGCTGGAAAC-3', rv 5'-ACGGCATATGCCATGA GCAATGCACCAGCCGGGAATCGAAC-3'; 3. fw 5'-TTGC TCATGGCATATGCCGTGTTTCAGAGCTATGCTGGAAAC-3', rv 5'-ATTTTAACTTGCTATTTCTAGCTCTAAAACAACCA TGTTCCGTAATCAGATGCACCAGCCGGGAATCGAAC-3')

that were cloned with a single Gibson Assembly reaction in a pCFD6 (Addgene plasmid no. 73915; RRID: Addgene\_73915) vector [26] which was previously digested with BbsI restriction enzyme.

After the constructs were created, they were injected into early embryos (*;Vas/Cas9*; for the *FoxP-*iB*-Gal4*, *FoxP-LexA* and *FoxP-KO* and *Integrase(x);;AttP2* for *UAS-t:grNA(4xFoxP)*). The resulting transformants were crossed two times with the balanced flies *w-;; D3/TM3, Sb*.

## 2.4. Immunohistochemistry

Three to 6 day-old adults were fixed in 4% paraformaldehyde (PFA) at 4°C for 2 h and dissected in 0.01% phosphate-buffered saline with Triton<sup>®</sup> X-100 detergent (PBST). For larval staining, third instar larvae were selected, dissected in 0.01% PBST and fixed in 4% PFA at room temperature (RT) for 30 min. Clean brains were washed three times in 0.01% PBST for a total time of 45 min and then blocked with 10% normal goat serum (NGS) for 1 h. Subsequently, the brains were incubated with the appropriate primary antibody for one to two nights at 4°C (table 2). After three washing steps of 15 min each, the brains were incubated with the secondary antibody (table 3) for 5–7 h at RT. After an additional 15 min washing step, the brains were placed on glass microscope slides and mounted with the antifade mounting medium Vectashield<sup>®</sup> (Vector Laboratories, Burlingame, CA).

## 2.5. Image acquisition and analysis

All images were acquired with a Leica SP8 confocal microscope (RRID: SCR\_018169), images were scanned at a frame size of 1024 × 1024 pixels at 200 or 100 Hz. The objectives were 20× dry and 20×/40×/60× oil immersion. Images were processed with IMAGEJ software (National Institutes of Health, Maryland, USA; RRID: SCR\_003070) [29], only general adjustments to colour, contrast and brightness were made. Cell counting was performed with IMARIS 9.0 (Oxford instruments, UK) software on *UAS-Stinger-GFP* stacks, using the tool for spots counting. For the *FoxP-*iB*-Gal4*/*FoxP-LexA* count (figure 4b), five brains were counted for each genotype at both larval (3rd instar) and adult (2–3 days old) stages. The colocalization analysis was performed with the ImageJ *Colocalization Threshold* tool (Tony Collins and Daniel James White) (figure 5b). The three-dimensional rendering (figure 12b) was performed with IMARIS 9.0 software on the *Drosophila* standard brain from <https://www.virtualflybrain.org>.

## 2.6. RT-qPCR

The knock-out efficiency was assessed using RT-qPCR (figures 1d and 4e). We extracted RNA from 20 flies for each genotype (*white<sup>-</sup>*, heterozygous mutant and homozygous mutant, both with a *white<sup>-</sup>* background), following the Tri-Fast<sup>™</sup> protocol from peqlab (a VWR company) (catalogue no. 30–2010). The RNA was subsequently transcribed into cDNA using the OneStep RT-PCR Kit from QIAGEN (catalogue no. 210212) with the following thermocycler programme: 42°C for 2 min, 4°C pause until manual restart at 42°C for 30 min, 95°C for 3 min and finally 10°C ∞. Subsequently, we performed the qPCR. Primer sequences were identical to those used by Mendoza *et al.* [18]. For the qPCR reaction, we used a Bio-Rad CFX Connect Real-Time PCR

**Table 2.** Complete list of the primary antibodies used in this study.

antigen	host	dilution	incubation	source	RRID
<i>Choptin-11</i>	mouse	1 : 500	1 night	DSHB	AB_528161
<i>ChAT</i>	mouse	1 : 250	1 night	DSHB	AB_528122
<i>ELAV</i>	rat	1 : 100	1 night	DSHB	AB_528218
<i>FoxP</i>	guinea pig	1 : 200	2 nights	Lawton <i>et al.</i> [21]	/
<i>GABA</i>	rabbit	1 : 250	2 nights	GeneTex	AB_2037030
<i>nc82</i>	mouse	1 : 500	1 night	DSHB	AB_2314866
<i>p-SMAD1/5</i>	rabbit	1 : 250	2 nights	Cell Signaling Technology	AB_491015
<i>REPO</i>	mouse	1 : 500	1 night	DSHB	AB_528448
<i>TH</i>	rabbit	1 : 500	1 night	Millipore	AB_390204

**Table 3.** Complete list of the secondary antibodies used in this study.

antigen	host	dilution	incubation	Source	RRID
Anti-guinea pig Cy <sup>TM</sup> 3	goat	1 : 200	7 h	Jackson ImmunoResearch	AB_2337423
Alexa-Fluor-Anti-mouse 555	goat	1 : 250	5 h	ThermoFisher Scientific	AB_2535844
Alexa-Fluor-Anti-rabbit 555	goat	1 : 250	5 h	ThermoFisher Scientific	AB_2535849
Alexa-Fluor-Anti-rat 555	goat	1 : 250	5 h	ThermoFisher Scientific	AB_2535855

Detection System thermocycler and the Bio-Rad CFX manager software to store and analyse the data. Every sample was run in triplicate in a 96-well plate in a total volume of 10  $\mu$ l. The mixture contained 5  $\mu$ l sybrGreen master mix (ORA<sup>TM</sup> qPCR Green ROX H Mix, 2X, from highQu, catalogue no. QPD0201), 0.5  $\mu$ l from each primer, 1  $\mu$ l of 1 : 10 diluted cDNA and 3  $\mu$ l H<sub>2</sub>O. As reference, we used the housekeeping gene *rp49* (*ribosomal protein 49*), while as a negative control we used the same reaction mix without cDNA. The qPCR reaction programme used was: 95°C for 2 min, 95°C for 10 s, 60°C for 10 s, 65°C for 30 s (from step 2 to 4  $\times$  39 rounds), 95°C for 10 s, and finally from 65°C to 95°C for +0.5°C/5 s. The experiments were repeated two to four times.

## 2.7. Behaviour

All behavioural experiments were performed in Buridan's paradigm (RRID: SCR\_006331) [30]. In this experiment, we analysed both temporal components of walking behaviour (often subsumed under 'general locomotion') and spatial components such as fixation of landmarks or the straightness of the walking trajectory. Buridan's paradigm (figure 6a) consists of a round platform with a diameter of 117 mm which is surrounded by a water-filled moat. The platform is situated at the bottom of a uniformly illuminated white cylinder, 313 mm in height and 293 mm in diameter [31]. Two black stripes are placed on the inside of the cylinder, opposite each other, serving as the only visual cues for the flies. Two day-old female flies were collected and their wings were clipped under CO<sub>2</sub> anesthesia. After one night recovery at 25°C, they were tested in Buridan's paradigm for 15 min (doi:10.17504/protocols.io.c7vzn5). The position of the fly is recorded by a camera (Logitech Quickcam Pro 9000) connected to a computer running our BuriTrack software (<http://buridan.sourceforge.net>).

The analysis software CeTrAn [31] (<https://github.com/jcolomb/CeTrAn>) extracts a variety of parameters from the scored trajectories. From the parameters extracted by CeTrAn, we used the temporal parameters median speed (the median of all instantaneous speed data points measured when the fly is walking), distance travelled, number of walks (sections of the trajectory which connect the platform areas closest to the two stripes) and activity time (fraction of time spent walking), as well as the spatial parameters stripe deviation (angular deviation of the fly's heading from the centre of the stripe in the frontal visual field) and meander (a measure of the tortuosity of the fly's trajectory). Transition plots visualize the areas on the platform that the flies most frequently visited. More details in [31].

For the experiment involving *Tub-Gal80<sup>ts</sup>* (figure 8e–h and 11a,b), flies were raised at 18°C, moved to 30°C for 12 h (embryos) or 48 h (pupae and adults) and subsequently left at 25°C for the rest of the development (embryos and pupae) or overnight for recovery (adults) before testing.

## 2.8. Statistical analysis

All graphs were created and statistical analysis was performed using GraphPad Prism 6 (GraphPad Software, Inc., California, USA; RRID: SCR\_002798) software. Sample variances were compared with an *F*-test. In the absence of significantly different variances, we used Student's *t*-tests (two-tailed) or one way ANOVAs followed by Tukey's post hoc test for multiple comparisons. If the *F*-test was significant at  $p < 0.005$  (see below), we used a Mann–Whitney *U*-test or a Kruskal–Wallis ANOVA followed by Dunn's post hoc test for multiple comparisons. Alpha values were set to 0.5%, in order to reduce the chances of false-positives, following the arguments detailed in [32], where BB is an author. Whenever null hypothesis significance testing was performed using the non-parametric tests, it is indicated in the figure legends. All other tests were performed using parametric tests.

The initial behavioural experiments (figure 6) were carried out with a sample size which, from experience, would be sufficient to detect medium to large effects, i.e.  $N \sim 20$ . We then used these results to perform a power analysis for the subsequent experiments. We found that effect sizes such as those exhibited in the speed, meander or stripe fixation parameters required a sample size of up to 18 to reach 80% statistical power at an alpha of 0.5% [32], while effects such as those in the activity time parameter would require up to 100 flies. We corroborated these analyses with Bayesian analyses, where the activity time parameter yielded a Bayes factor below one, while the other effects yielded Bayes factor values beyond 100. Therefore, we set the target sample size for all subsequent Buridan experiments to 18 and  $p < 0.005$  was considered significant. Data are expressed as averages  $\pm$  s.e.m. or averages  $\pm$  s.d., and each case is indicated in the legend of each figure.

## 3. Results

### 3.1. FoxP-iB expression in the *Drosophila* brain

The *FoxP* transcription factor binds DNA with the forkhead (FH) box domain (figure 1a, yellow boxes; raw data deposited at doi:10.6084/m9.figshare.12607700). The gene consists of seven introns and eight exons. The FH box is split into different segments spanning exons 6, 7 and 8. The last two exons (7 and 8) are subjected to alternative splicing, leading to two different protein isoforms: isoform A (*FoxP-iA*), which results from splicing exon 6 to exon 7, and isoform B (*FoxP-iB*) where instead exon 8 is spliced to exon 6. A third, intron-retention isoform is transcribed by failing to splice the intron between exon 6 and 7 out (*FoxP-iIR*). While the first two isoforms contain a complete and putatively functioning FH box (with 10 amino acids different between the two; figure 1a, dashed box), the putative FoxP-iIR FH box appears to be truncated due to a stop codon in the intron sequence (figure 1a, red line), putting the transcription factor function of this isoform in doubt. Of the three FoxP isoforms, *FoxP-iB* was most directly associated with the learning phenotype discovered by Mendoza *et al.* [18]. Therefore, we inserted the sequence of the yeast transcription factor Gal4 into exon 8, the exon which is exclusive to *FoxP-iB* (figure 1a). This insertion leads to the expression of the Gal4 transcription factor only in *FoxP-iB* positive cells. At the same time, the insertion also disrupts the FH box DNA-binding domain of the *FoxP* gene, putatively preventing the FoxP protein to act as a transcription factor, effectively mutating the gene for this function.

Observing Gal4 expression with different green fluorescent proteins (GFPs) under control of the UAS promoter (to which Gal4 binds), revealed that *FoxP-iB* is expressed throughout the whole development of the fly, from embryo (data deposited at doi:10.6084/m9.figshare.12607652) to adult, in both brain and ventral nerve cord (VNC) (figure 1b). In 3rd instar larvae, we observe expression in the central brain (but not in the optic lobes) and in the anterior portion of the VNC. In the adult nervous system, the main neuropil expression domains comprise protocerebral bridge, gnathal ganglia (suboesophageal zone), vest, saddle, noduli and superior medial protocerebrum. GFP-positive cell body clusters could be found in the cortex of the central brain and around the optic lobes (figure 1b).

We next validated the expression pattern of our *iB*-specific driver line to the staining of an available isoform-unspecific

polyclonal antibody [21]. We observed complete colocalization of the driver line with the antibody staining in both larvae and adults, i.e. there were no GFP-positive cells that were not also labelled by the FoxP antibody (figure 1c). The cells only stained for the FoxP antibody and not for GFP are presumably cells expressing the other *FoxP* isoforms (*FoxP-iA* and *FoxP-iIR*, figure 4). Notably, in contrast to previous reports [34,35] but consistent with [20], we did not detect any *FoxP* expression in mushroom body (MB) neurons, neither with our driver line, nor with the antibody.

Postulating that our transgene disrupted expression of the *FoxP* gene, we measured mRNA levels of all three isoforms with RT-qPCR (figure 1d). With one of the primers placed over the Gal4 insertion site, we observed approximately half the wild-type *FoxP-iB* expression levels in heterozygous animals, while wild-type *FoxP-iB* expression was essentially abolished in the homozygous transgenes. We did not observe any significant changes in the other two isoforms. However, this disruption of the *FoxP-iB* isoform did not have an effect on the development of the *FoxP*-positive neurons, as both heterozygous and homozygous *FoxP-iB-Gal4* mutants showed the same number of GFP-labelled cell nuclei (data deposited at doi:10.6084/m9.figshare.12932705).

### 3.2. FoxP-iB is expressed in a variety of neurons, but not glia

With *FoxP* involved in learning and expression patterns suggesting neuronal expression (figure 1), we investigated whether the observed expression was exclusively neuronal, or if there were also *FoxP-iB* expressing glial cells. Therefore, we stained 3rd instar larva and adult brains with antibodies against ELAV (neuronal marker) and REPO (glial marker). At both developmental stages, the two stainings reveal exclusive *FoxP-iB*-mediated GFP colocalization with ELAV without any colocalization with REPO (figure 2a,b; raw data deposited at doi:10.6084/m9.figshare.12607706), suggesting that *FoxP-iB* is expressed exclusively in neurons. These data are consistent with results published previously [20,36], validating the methods employed here.

We next investigated in more detail the types of neurons in which *FoxP-iB* is expressed. Using a variety of antibodies (figure 3; raw data deposited at 10.6084/m9.figshare.12607712) used as markers for different neuronal cell types we detected *FoxP-iB* expression in most of the cell types investigated. For technical reasons, we stained adult brains only with the anti-TH antibody, while the remaining markers were used on larval nervous systems. Extensive colocalization was observed with p-SMAD1/5 (a motor neuron marker) in the VNC but not in the central brain (CB) (figure 3a). Some *FoxP-iB* neurons were positive for ChAT (cholinergic) or GABA (inhibitory) both in the VNC and in the CB (figure 3b,c). Finally, a few *FoxP-iB* positive neurons were found to colocalize with tyrosine hydroxylase (dopaminergic neurons) in the CB only (figure 3d). These data are consistent with the study performed by Schatton *et al.* [37] in honeybees where they found colocalization between AmFoxP-positive neurons and GABAergic, cholinergic and monoaminergic markers. No colocalization was instead found in photoreceptor cells stained with Chaoptin (data deposited at doi:10.6084/m9.figshare.12607643), a marker for photoreceptor cells [38].

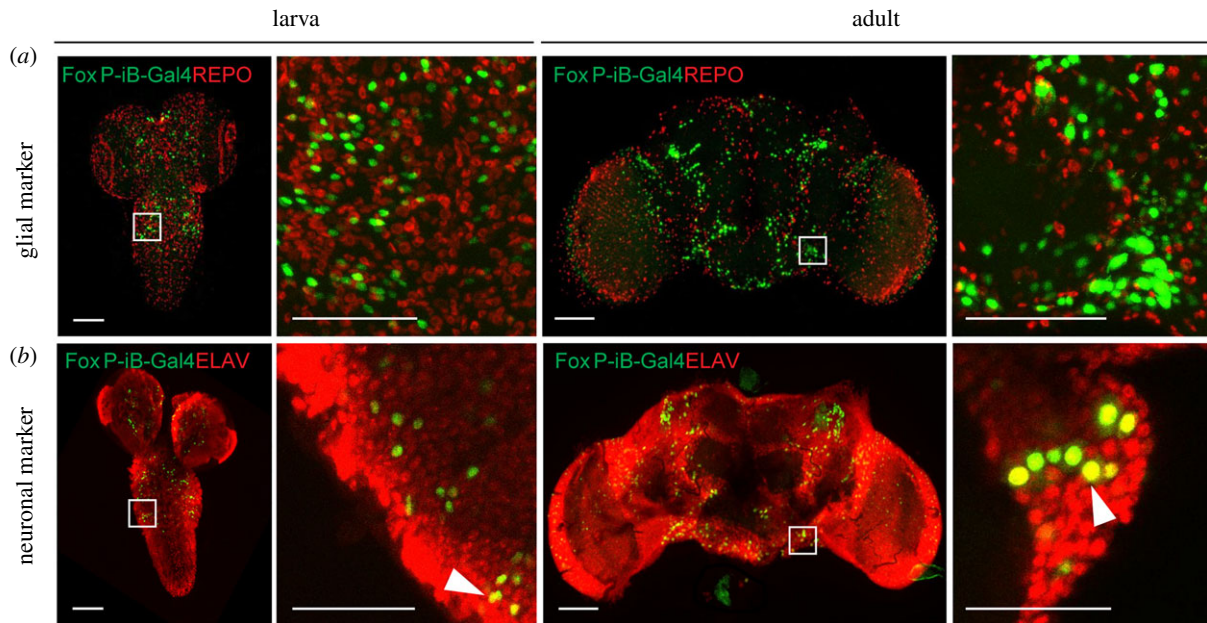


**Figure 2.** Only neurons, not glia, are expressing *FoxP-iB* in the *Drosophila* brain. Immunohistochemistry on *FoxP-iB-Gal4 > Stinger-GFP* flies with REPO (glia, *a*) and ELAV (neurons, *b*) markers. Note the lack of colocalization of *FoxP-iB* driven GFP with the glial marker in both 3rd instar larvae and adult brains (*a*). By contrast, exclusive colocalization of *FoxP*-driven GFP with the neuronal marker was observed in both developmental stages (white arrowheads indicate typical examples). Scale bars: 50  $\mu$ m.

### 3.3. *FoxP-iB* is expressed in a subset of *FoxP*-expressing neurons

As the antibody staining against the FoxP protein indicated more cells expressing FoxP than our *FoxP-iB*-specific driver line was reporting (figure 1*b*), we created a second driver line, designed to drive expression in all FoxP cells, irrespective of isoform. We inserted a sequence for the bacterial LexA [39] transcription factor into exon 3 (figure 4*a*; raw data deposited at doi:10.6084/m9.figshare.12607730). Comparing *Stinger-GFP* expression from each driver line revealed a more expansive pattern for the isoform-unspecific driver (figure 4*b*), one that matches very well with the FoxP antibody staining (figure 1*b*). This visual impression was corroborated by a quantification of stained nuclei comparing between both drivers (figure 4*c*). This quantification allowed us to trace the proliferation of FoxP cells from around 500 in 3rd instar larvae to around 1800 in 3 day-old adults. By contrast, there are only about 300 cells expressing *FoxP-iB* in the 3rd larval instar and only around 1300 in 3 day-old adults. We noticed that the largest differences in terms of cell number between *FoxP-LexA* and *FoxP-iB-Gal4* flies (both larvae and adults) were found in the CB, while the VNC numbers differed considerably less. Taken together, in 3rd instar larvae and in 3 day-old adults, 66% and 65%, respectively, of the total number of *FoxP* neurons in the *Drosophila* nervous system express *FoxP-iB*. As with our previous insertion, also this one was expected to disrupt expression of the *FoxP* gene. To investigate the extent of this disruption on the mRNA level, we again performed RT-qPCR. As expected, this insertion affected all isoforms. In heterozygous flies, the expression level was increased, while in homozygous flies it was decreased (figure 4*e*). It is important to note that here, in contrast to the *FoxP-iB* insertion, all primers are binding sequences downstream of the insertion site (figure 1*a,d*) and so are amplifying all transcripts, with or without the insertion. Possibly, the FoxP protein is involved in its own regulation such

that in heterozygotes, the missing gene copy leads to a compensatory increase in transcription rate, but in homozygous mutant animals without any FoxP protein, only basal expression levels remain.

In order to directly compare the expression patterns of our two driver lines, we used them to drive reporter genes fluorescing at different wavelengths (i.e. *LexAop-RFP;UAS-CD8-GFP*) and analysed their patterns in adults (figure 5; raw data deposited at doi:10.6084/m9.figshare.12607763). In this way, we labelled all *FoxP*-expressing neurons red and neurons that specifically expressed *FoxP-iB* green. We used the 'Colocalization Threshold' tool from ImageJ, which computes false colours to enhance the comparison between the two driver lines and let the differences stand out (see Material and methods). The other two isoforms are expressed in additional areas (the antennal lobe, the lobula, the fan-shaped body and the posterior ventrolateral protocerebrum) compared to *FoxP-iB* expression (figure 5*a*, red arrowheads; figure 5*b*, blue areas).

We also crossed this *FoxP-LexA* line with *LexAop-RFP;UAS-CD8-GFP* and *Tdc2-Gal4* to investigate any potential tyraminergetic or octopaminergic *FoxP* neurons, but despite a close proximity between the two cell types, no colocalization was found (data deposited at doi:10.6084/m9.figshare.12607670).

### 3.4. *FoxP-iB* knock-out flies show a multitude of behavioural abnormalities

Mutations in the *FoxP* gene do not only affect operant self-learning, for instance, different alleles also affect flight performance and other locomotion behaviours to different degrees [18,20,21]. Because of the *FoxP* pleiotropy affecting various innate motor behaviours independently from motor learning, we turned to Buridan's paradigm [30,31] as a powerful tool to measure several locomotor variables. Buridan's paradigm allows us to test a broad panel of behavioural parameters covering temporal parameters such as speed or general activity

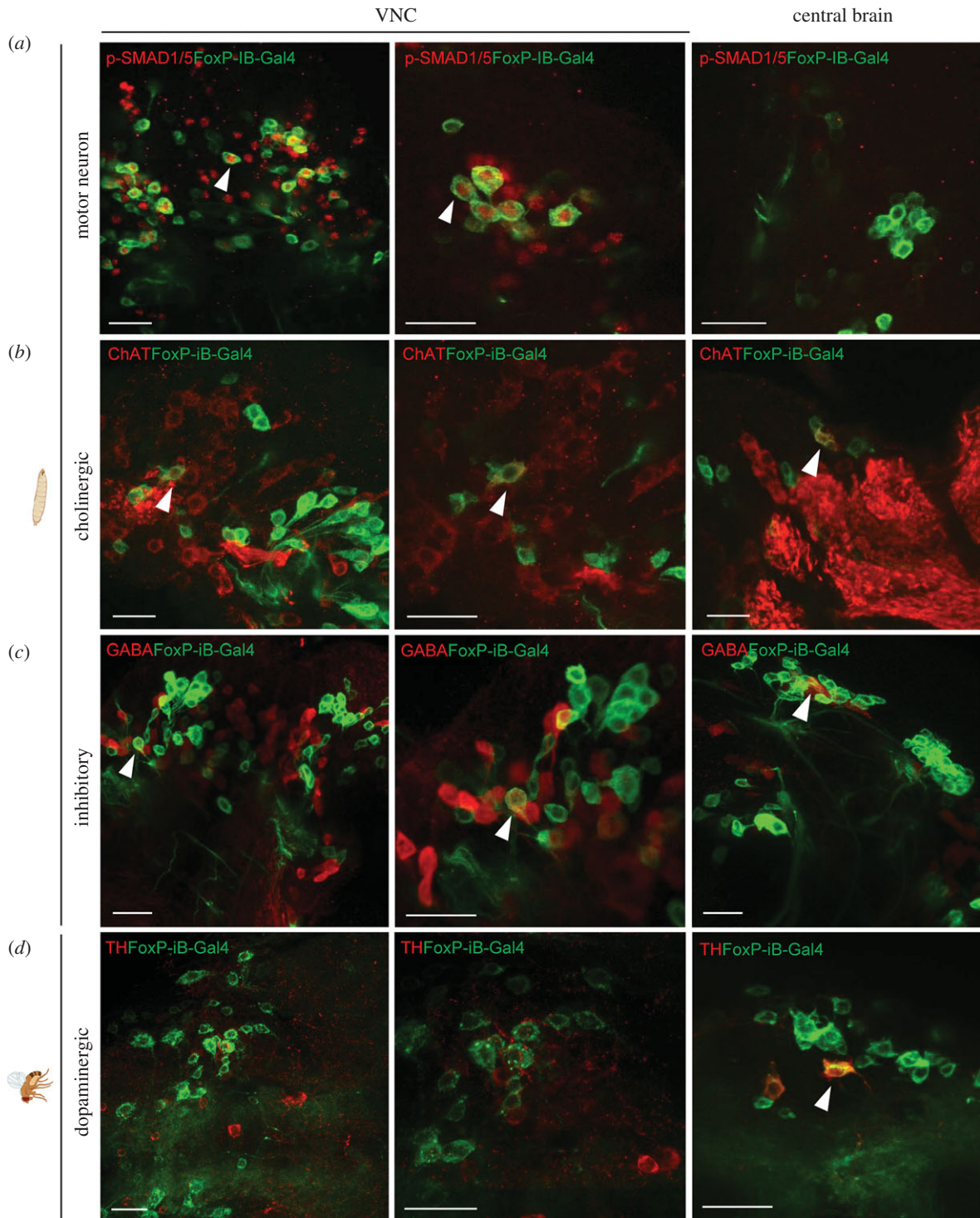


**Figure 3.** *FoxP-iB* is expressed in various types of neurons. Immunohistochemistry on *FoxP-iB-Gal4 > CD8-GFP* larvae and adults using different antibodies. (a) Some of the *FoxP-iB* positive neurons colocalize with p-SMAD1/5 in the VNC but not in the central brain. (b,c) *FoxP-iB* neurons positive for ChAT or GABA have been found in both the VNC and CB. (d) Only few *FoxP-iB* neurons colocalize with TH and only in the CB. White arrowheads indicate examples of colocalization. Scale bars, 25 μm. (a–c) larvae; (d) adult flies.

time and spatial parameters such as the straightness of a fly's trajectory (meander) or the degree to which the animal is heading towards one of the two vertical landmarks (stripe fixation; figure 6a).

With our insertions constituting novel alleles impairing *FoxP* expression (figures 1 and 4), we started by testing the heterozygous and homozygous driver strains without any effectors.

Consistent with previous findings of impaired locomotor behaviour in *FoxP* manipulated flies [18,20,21] and the qPCR results showing reduced *FoxP* expression (figure 1d), our

*FoxP-iB-Gal4* insertion shows abnormalities in Buridan's paradigm both in temporal and in spatial parameters (figure 6; raw data deposited at doi:10.6084/m9.figshare.12607769). While the homozygous flies walked more slowly, spent more time at rest and fixed the stripes less strongly than wild-type control flies, heterozygous flies only differed from wild-type flies in their stripe fixation (figure 6c). With different effect sizes in each parameter, we selected two representative parameters each for the temporal and the spatial domain, respectively, for comparison of all subsequent lines: walking speed, activity time, meander and stripe fixation.

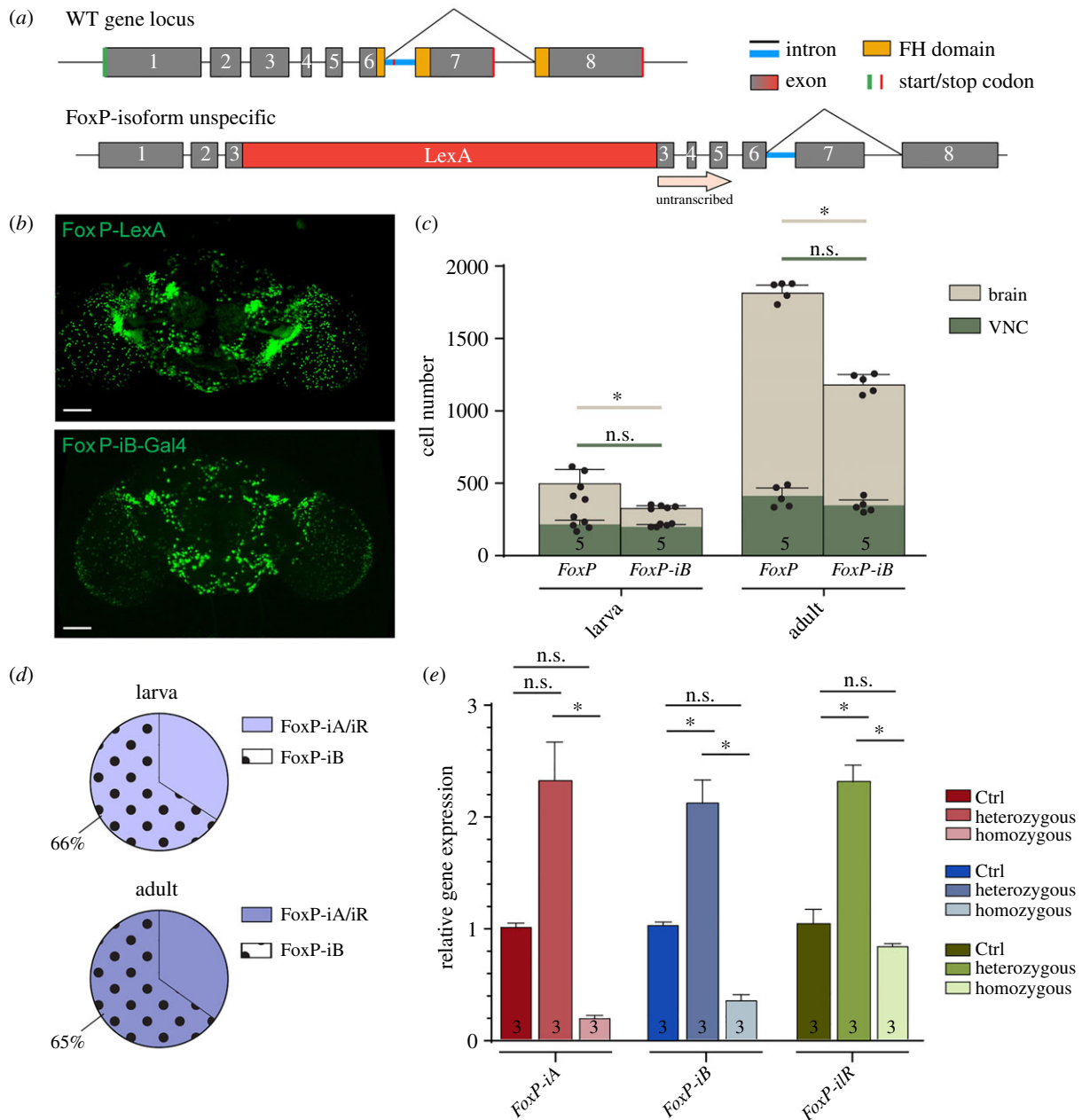


**Figure 4.** *FoxP-iB* is expressed in a subset of *FoxP*-expressing neurons. (a) Schematic representation of the *FoxP* gene locus after LexA insertion. This is an isoform-unspecific construct with the insertion of a LexA sequence in exon 3. (b) Expression pattern of *FoxP-LexA* and *FoxP-iB-Gal4* driving *Stinger-GFP*. (c) Cell counting performed with IMARIS on *FoxP-LexA* and *FoxP-iB-Gal4* > *Stinger-GFP* (3rd instar larvae and 3 day-old adults) in both brain and VNC. (d) Pie charts that summarize the results from (c). (e) RT-qPCR on *FoxP-LexA* flies (control, hetero- and homozygous flies). Data are expressed as means  $\pm$  s.d. in (c) and as means  $\pm$  s.e.m. in (e). \* $p < 0.005$ . Scale bars, 50  $\mu$ m.

Because our insertion is located in the same exon as the insertion in the *FoxP*<sup>3955</sup> mutant, we tested the *FoxP*<sup>3955</sup> mutant flies in Buridan's paradigm and found changes in several temporal parameters, similar to those observed in our driver line (figure 6d). However, for the spatial parameters (stripe deviation and meander) only stripe fixation appears normal in these flies, the increased meander indicates that the flies have problems walking straight, despite clearly walking towards the stripes. Thus, in addition to the deficits in operant self-learning and flight performance as reported previously [18], the *FoxP*<sup>3955</sup> mutant flies are also deficient in several temporal and one spatial parameter of walking behaviour in Buridan's paradigm. This walking phenotype is consistent with previous findings of walking deficits associated with *FoxP* manipulations [20,21], but was not detected in a previous publication where tests for walking deficits had been performed [35].

#### 4. Knocking out all *FoxP* isoforms has similar effects as *FoxP-iB* knock-out

With such dramatic motor alterations when only *FoxP-iB*, which is expressed in about 65% of all *FoxP*-positive neurons (figure 4), is removed (figure 6), it is interesting to study the effects of removing the remaining isoforms for a complete *FoxP* knock-out. To avoid unwanted potential side-effects of expressing a different protein in its stead, we created a third fly line where the entire second exon is removed together with parts of exons 1 and 3. We validated this mutant with the polyclonal antibody we used before (figure 1). While the antibody detected the *FoxP* gene product in control flies, there was no signal in our homozygous knock-out flies (figure 7a,b; raw data deposited at doi:10.6084/m9.figshare.12607796).

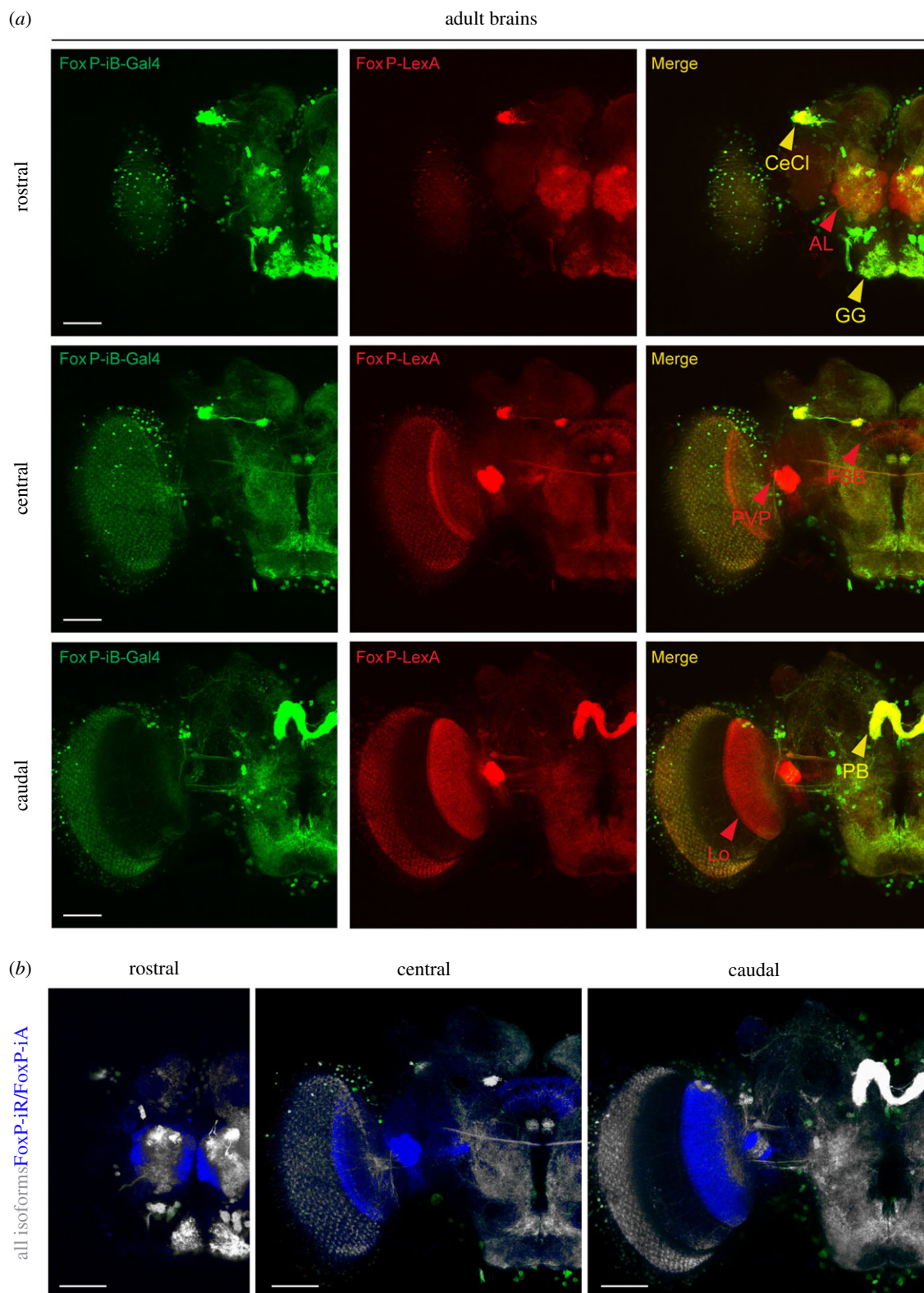


**Figure 5.** Comparison of *FoxP*-isoform expression patterns. (a) Confocal images of adult brains expressing *FoxP-iB-Gal4* > *CD8-GFP* (green) and *FoxP-LexA* > *CD8-RFP* (red). (b) Difference rendering (blue) indicating areas expressing only non-iB isoforms. AL, antennal lobe; PVP, posterior ventrolateral protocerebrum; FSB, fan-shaped body; Lo, lobula; ccd, cell cluster; GG, gnathal ganglion; PB, protocerebral bridge. Scale bars, 50  $\mu$ m.

Analogous to the behavioural characterization in the *FoxP-iB* insertion line, we tested both heterozygous and homozygous *FoxP-KO* deletion mutants in Buridan's paradigm (figure 7c–f). The results of this experiment closely resemble the ones from the *FoxP-iB-Gal4* insertion line, with homozygous mutants being both significantly less active (figure 7c) and fixating the stripes less strongly than the heterozygous mutants and the wild-type controls (figure 7d,e). For this allele, the heterozygous *FoxP-KO* mutants show higher

values for all temporal parameters compared to the wild-type controls, while there is no difference in stripe deviation. This trend was already observed in *FoxP-iB* mutants but failed to reach statistical significance. Thus, the *FoxP-KO* allele exhibits differential dominance, with recessive modes of inheritance in some traits and, e.g. overdominance in others. A direct comparison of the data from the two homozygous alleles (*FoxP-iB* and *FoxP-KO*) showed no significant differences (figure 7f). Thus, removing the other *FoxP* isoforms

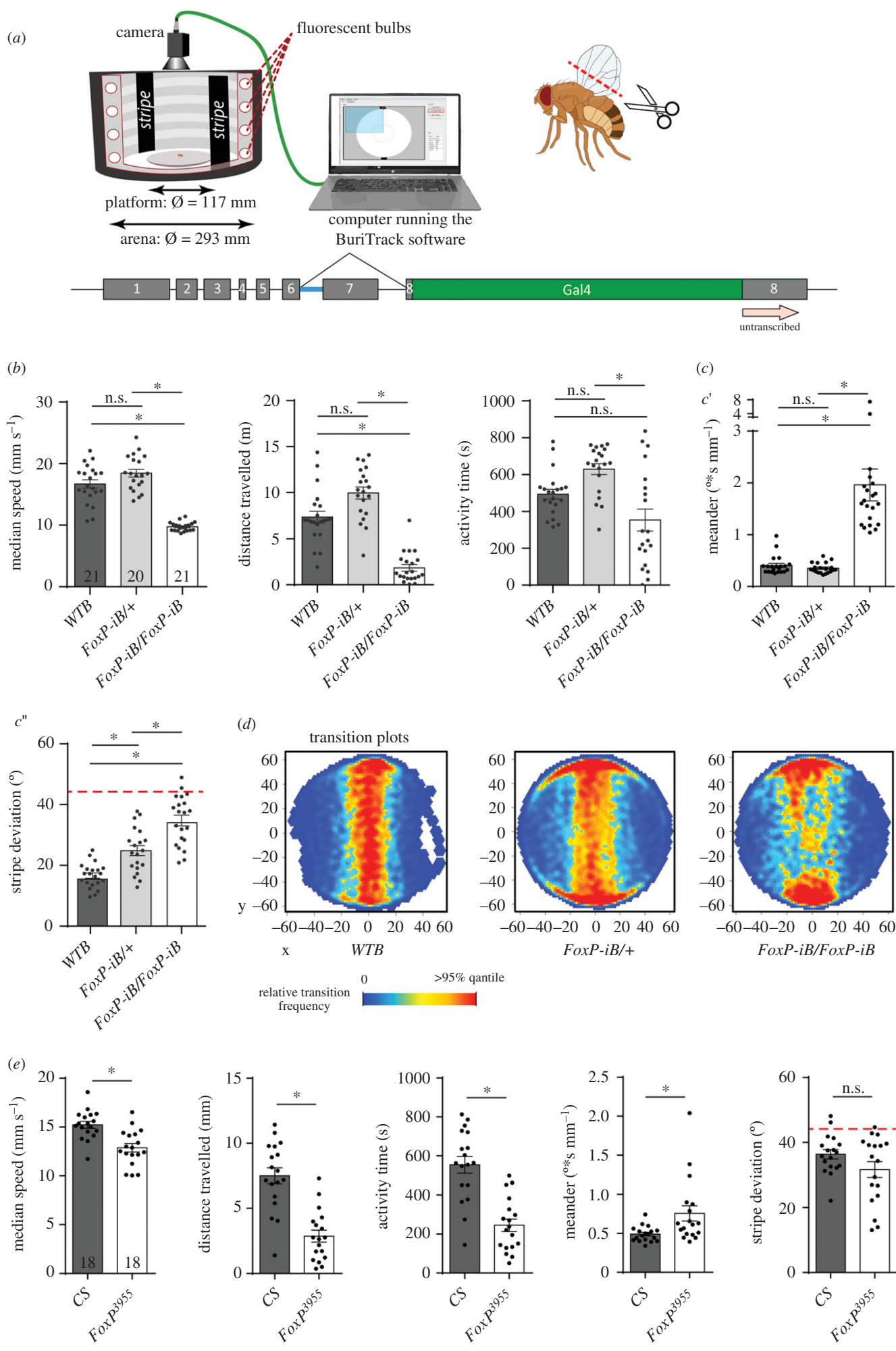


Figure 6. (Caption continued.)

**Figure 6.** (Continued.) *FoxP-iB* mutant flies are impaired in several parameters in Buridan's paradigm. (a) Schematic of Buridan's paradigm. A fly with shortened wings is put in the centre of a platform inside a circular arena with two opposing black stripes on the walls. A camera records the position of the fly and the BuriTrack software stores the position data for later analysis with CeTrAn. (b) Temporal parameters. Median speed denotes the instantaneous speed when a fly is walking. Activity time denotes the time spent walking. Distance traveled measures the distance covered by the fly during the experiment. Non-parametric tests for walking speed and activity time. (c) Spatial parameters. Meander is a measure for the tortuosity of a fly's trajectory. Stripe deviation measures the angular deviation from heading towards the centre of the stripe to which the fly is oriented. Red dashed line indicates angular stripe deviation of a random walk. Non-parametric test for meander. (d) The transition plots show the distribution of the platform locations that the flies transitioned through. (e) Temporal and spatial parameters from CS and *FoxP*<sup>3955</sup> mutant flies in Buridan's paradigm are largely consistent with those from the *FoxP-iB* knock-out. Non-parametric test for meander. \* $p < 0.005$ .

had few effects beyond the consequences of removing only *FoxP-iB* alone.

#### 4.1. Local and conditional *FoxP* knock-out (*FoxP-CKO*)

Given the patchy expression pattern of *FoxP* in the fly's nervous system (figures 1–5) and the grave consequences for behaviour in Buridan's paradigm if it is manipulated (figures 6 and 7), we sought to investigate when and where *FoxP* is required for normal walking behaviour. To this end, we designed a fourth fly strain which carries a UAS-controlled effector (figure 8a; raw data deposited at doi:10.6084/m9.figshare.12607805). The four guide RNAs (gRNA) each target a different section of the *FoxP* gene (see Material and methods). If expressed together with the endonuclease Cas9, this effector efficiently mutates the targeted gene [26,40]. We validated this approach by driving both our gRNAs as well as Cas9 using the pan-neuronal *elav-Gal4* driver and monitoring *FoxP* expression with the *FoxP* antibody used before (figure 8b). Flies with this pan-neuronal excision of the *FoxP* gene (*FoxP-CKO*) were also tested in Buridan's paradigm and showed even more severe impairments than flies homozygous for a constitutive deletion of the gene (figure 8c). In fact, the mutated flies walked so little, that analysis of spatial parameters was not meaningful (figure 8d). To allow for temporal control of transgene expression, we also validated the use of the temperature-sensitive suppressor of Gal4, Gal80<sup>ts</sup> (figure 8e). The constitutively expressed Gal80<sup>ts</sup> prevents Gal4 from activating transcription of the UAS-controlled transgenes until the temperature is shifted from 18°C to 30°C, at which point the repressor becomes inactivated and Gal4-mediated transcription commences [23,24]. Using this system to drive gRNA/Cas9 expression for 12 h in the embryo phenocopies both the mutant and the local phenotypes not only on the protein (figure 8f), but also on the behavioural level (figure 8g,h). In both experiments, the effects of the manipulations were so severe, that it was not possible to reach the target sample size of 18.

#### 4.2. Local *FoxP-KO*: brain regions and neuron types

Recently, Linneweber *et al.* [41] described the consequences of silencing dorsal cluster neurons (DCNs) on stripe fixation behaviour in Buridan's paradigm. The *FoxP-iB* expression pattern suggests that at least some of these DCNs express *FoxP* (figure 1). Comparing our isoform-unspecific *FoxP-LexA* expression pattern with that of the *atonal-Gal4* line used to drive expression in DCNs [42], we observed substantial overlap (figure 9a; raw data deposited at doi: 10.6084/m9.figshare.12607811). Therefore, we used *ato-Gal4* to excise the *FoxP* gene specifically in DCNs. Remarkably, this manipulation

did not have any effect on the flies' behaviour in Buridan's paradigm (figure 9b).

The insect MBs are not only known as a centre for olfactory learning and memory [e.g. 43–50], they are also involved in the temporal and spatial control of locomotor activity [e.g. 51–60]. In addition, Castells-Nobau *et al.* [20] found a subtle structural phenotype in a sub-section of the MBs without detectable *FoxP* expression in the MB Kenyon cells themselves. Finally, there are two reports that expressing anti-*FoxP* RNAi constructs exclusively in the MBs can have behavioural effects [34,35]. For these reasons, despite neither [20] nor us being able to detect any *FoxP* expression in the MBs (and current RNAi constructs fail to knock down *FoxP* mRNA, see below), we deleted the *FoxP* gene from MB Kenyon cells using the *ok107-Gal4* driver and tested the flies in Buridan's paradigm. We did not detect any differences to control flies in these experiments (figure 9c).

There are two reasons for knocking out *FoxP* in motor neurons, besides *FoxP* expression there (figure 3): first, networks of motor neurons in the VNC control movement patterns and walking is directly affected by our manipulations so far (figures 6 and 7). Second, motor neurons were shown to be important for the type of operant self-learning that also requires *FoxP* [61]. Driving expression of gRNA/Cas9 with either of two motor neuron-specific driver lines (*D42-Gal4* and *C380-Gal4*) led to a significant alteration in locomotor activity in Buridan's paradigm, both for spatial and for temporal parameters (figure 10a,b; raw data deposited at doi:10.6084/m9.figshare.12607823).

Perhaps the most prevalent *FoxP* expression can be observed in the protocerebral bridge (figure 1). The driver line *cmpy-Gal4* targets the protocerebral bridge specifically and drives expression in *FoxP*-positive neurons (figure 10c). Removing the *FoxP* gene exclusively in these neurons led to a significant reduction of locomotor activity (figure 10d) as well as a reduction in stripe fixation and to more tortuous trajectories (figure 10e). In fact, the stripe deviation increased to an extent that it can no longer be distinguished statistically from a random walk at the 0.5% level (Wilcoxon signed rank test against 45°,  $V = 33$ ,  $p = 0.02$ ).

#### 4.3. Conditional *FoxP-KO*: developmental stages

With *FoxP* being a transcription factor active throughout development and particularly important during pupal development [20,62], we knocked out *FoxP* in all neurons by adding the Gal4 repressor Gal80<sup>ts</sup> to our pan-neuronal *FoxP-CKO* (figure 11a; raw data deposited at doi:10.6084/m9.figshare.12607838) and treating the flies with a 48 h 30°C heat treatment during the early pupal stage. This regime did not affect walking behaviour in Buridan's paradigm (figure 11b). Shifting the temperature treatment to immediately after eclosion also did not affect the flies'

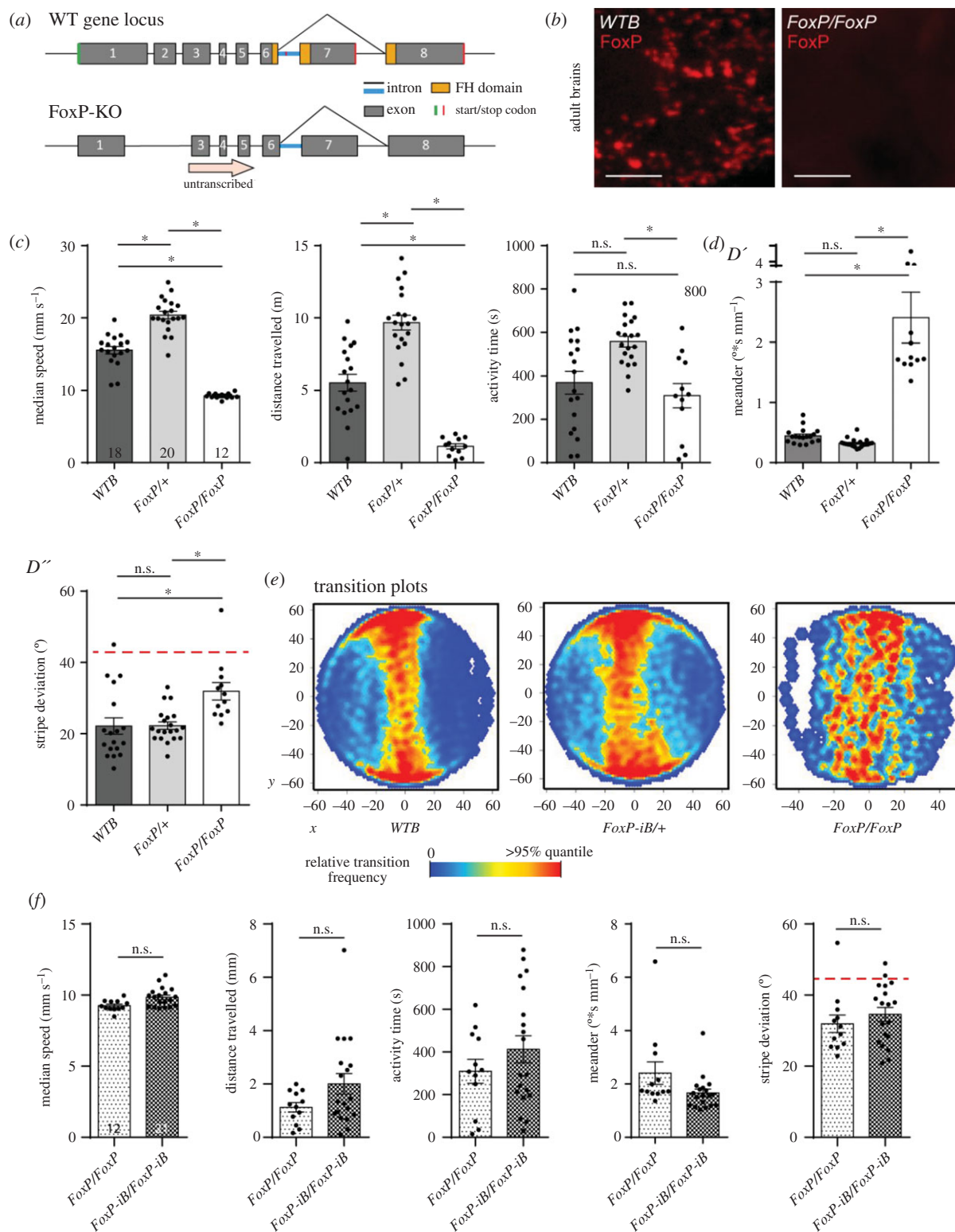


**Figure 7.** Deleting the entire *FoxP* gene has similar consequences in Buridan's paradigm as deleting only *FoxP-iB*. (a) Schematic of the deletion (*FoxP-KO*) and the wild-type (*WT*) gene locus. (b) Immunohistochemistry staining for the *FoxP* gene product in wild-type and *FoxP-KO* mutant brains. (c) Temporal parameters. See figure 6 and Material and methods for definitions. Note the overdominance of the heterozygous *FoxP-KO* flies. Stripe deviation (d) and transition plots (e) show weaker stripe fixation of homozygous *FoxP-KO* flies. (f) Comparing *FoxP-KO* and *FoxP-iB* flies reveal only a small difference in walking speed. Non-parametric tests for distance travelled and meander. \* $p < 0.005$ . Scale bars, 25  $\mu\text{m}$ .

behaviour in Buridan's paradigm (figure 11c). Taken together, these data indicate that *FoxP* is required for the proper development of, for instance, motor neurons and protocerebral bridge neurons, but once these circuitries are in place, *FoxP* expression does not appear to have any immediate mechanistic role in locomotion anymore.

## 5. Discussion

We have edited the genomic locus of the *Drosophila* *FoxP* gene in order to better understand the expression patterns of the *FoxP* isoforms and their involvement in behaviour. We have discovered that the isoforms differ with respect to

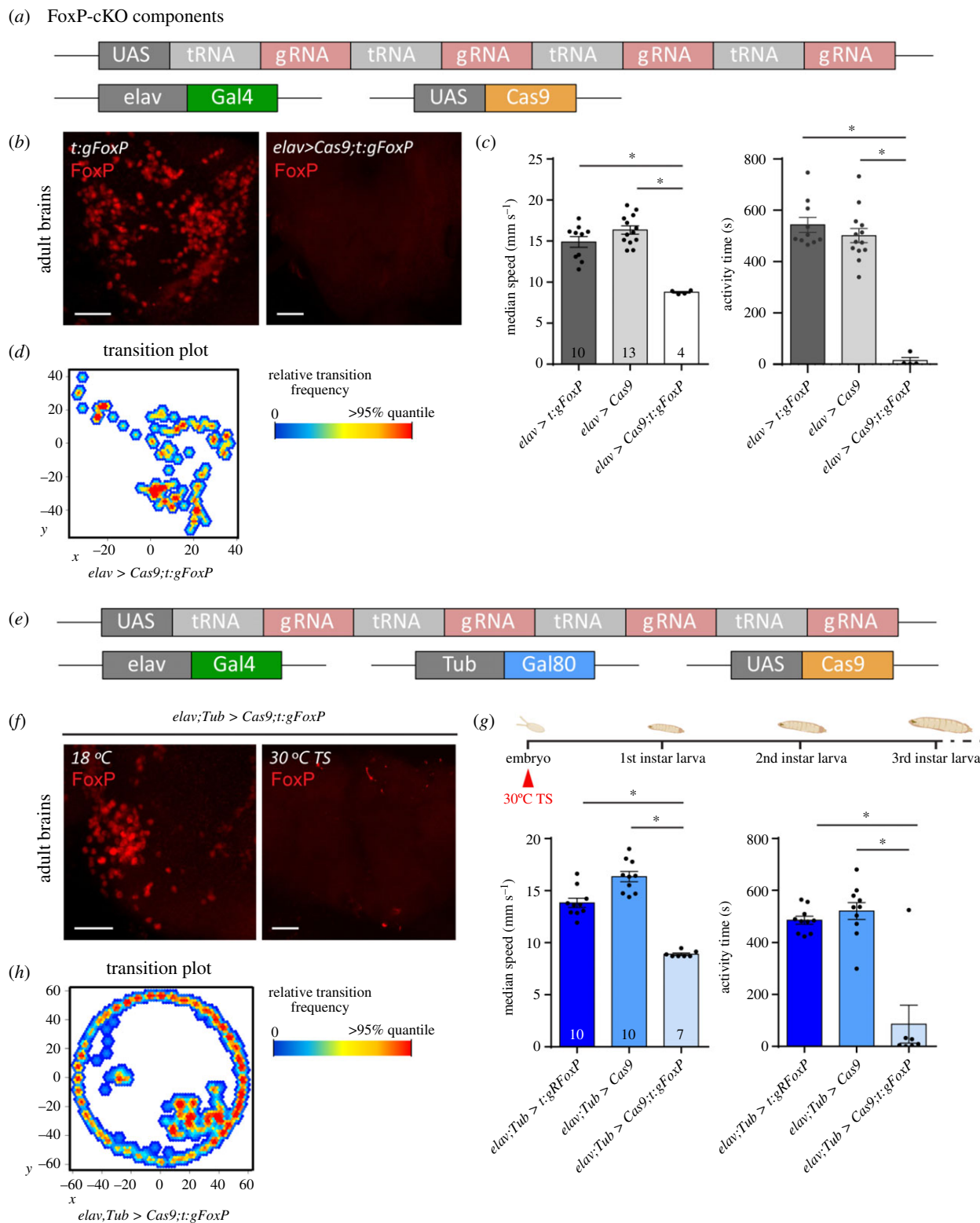


**Figure 8.** Local and conditional *FoxP* gene knock-out mimics mutant phenotype. (a) Construct schematic of the effector (UAS) line we created, together with the *elav* driver line and *Cas9* effector. (b) Immunohistochemistry on adult brains of the effector control line (left), and of the experimental cross (right). Driving expression of our gRNA construct with *elav-Gal4* leads to a highly efficient *FoxP* gene knock-out. (c) This knock-out is also validated in Buridan's paradigm, where the experimental flies show strongly reduced locomotor activity. Non-parametric test for speed. (d) Transition plot showing the reduced activity of *FoxP*-cKO flies. (e) Schematic of the used transgenic elements. Gal80<sup>15</sup> inhibits Gal4 under 30°C. (f) Induction of panneural gRNA expression in the embryo eliminates *FoxP* expression as tested with a *FoxP* antibody (right) compared to uninduced controls (left). (g, h) Inducing panneural gRNA expression in the embryo also leads to similar locomotor defects as observed in mutants and in flies expressing the gRNAs without temporal control. Non-parametric tests for both parameters. \**p* < 0.005. Scale bars, 25 μm.

their expression in neuronal tissue. For instance, we found isoform B (*FoxP-ib*) expression in neuropil areas such as the superior medial protocerebrum, the protocerebral bridge, the noduli, the vest, the saddle, the gnathal ganglia and the

medulla, while areas such as the antennal lobes, the fan-shaped body, the lobula and a glomerulus of the posterior ventrolateral protocerebrum contain other *FoxP* isoforms but not isoform B (summarized in figure 12) (raw data

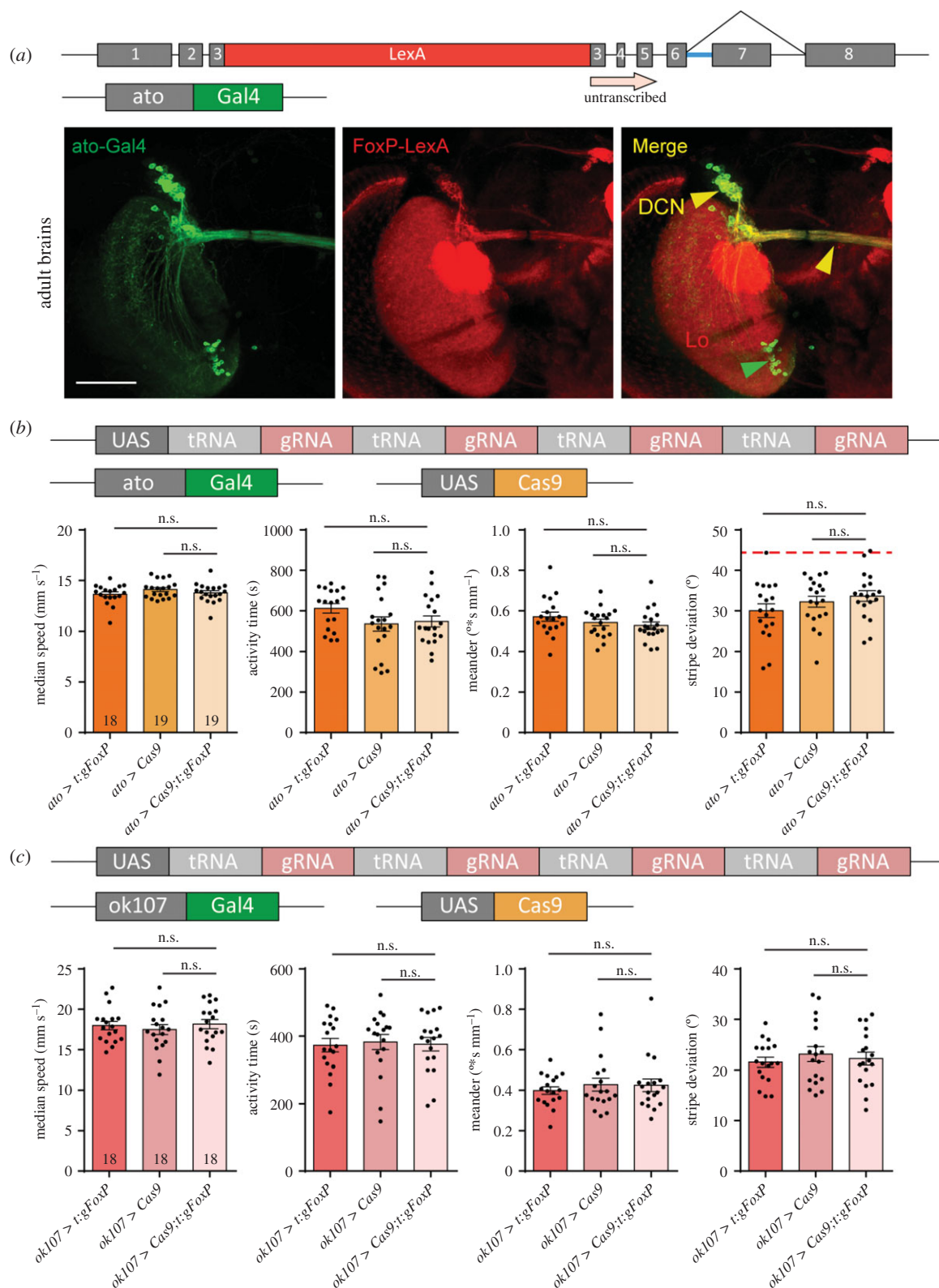


**Figure 9.** Local *FoxP*-KO shows no effect in DCN or mushroom bodies. (a) Immunohistochemistry showing *FoxP-LexA* expression in the adult brain compared to the expression of the *ato-Gal4* driver. DCN, dorsal cluster neurons; Lo, lobula. Scale bars, 50  $\mu\text{m}$ . (b) Temporal and spatial parameters from Buridan's experiment show no effects of knocking out the *FoxP* gene in DCN using the *ato-Gal4* driver. (c) Knocking out the *FoxP* gene in the mushroom bodies using the *ok107-Gal4* driver has no effect on either spatial or temporal parameters in Buridan's paradigm.

deposited at doi:10.6084/m9.figshare.12607862). We also corroborated previous results [20] that *FoxP* is expressed in a large variety of neuronal cell types (figure 3). Our genomic manipulations created several new alleles of the *FoxP* gene which had a number of behavioural consequences that mimicked other, previously published alleles [20]. Specifically, we found that constitutive knock-out of either *FoxP-IB* alone or of all *FoxP* isoforms affects several parameters of

locomotor behaviour, such as walking speed, the straightness of walking trajectories or landmark fixation (figures 6 and 7). We discovered that mutating the *FoxP* gene only in particular neurons can have different effects. For instance, knocking *FoxP* out in neurons of the dorsal cluster (where *FoxP* is expressed) or in MB Kenyon cells (where neither we nor [20] were able to detect *FoxP* expression) had no effect in Buridan's paradigm (figure 9), despite these neurons being

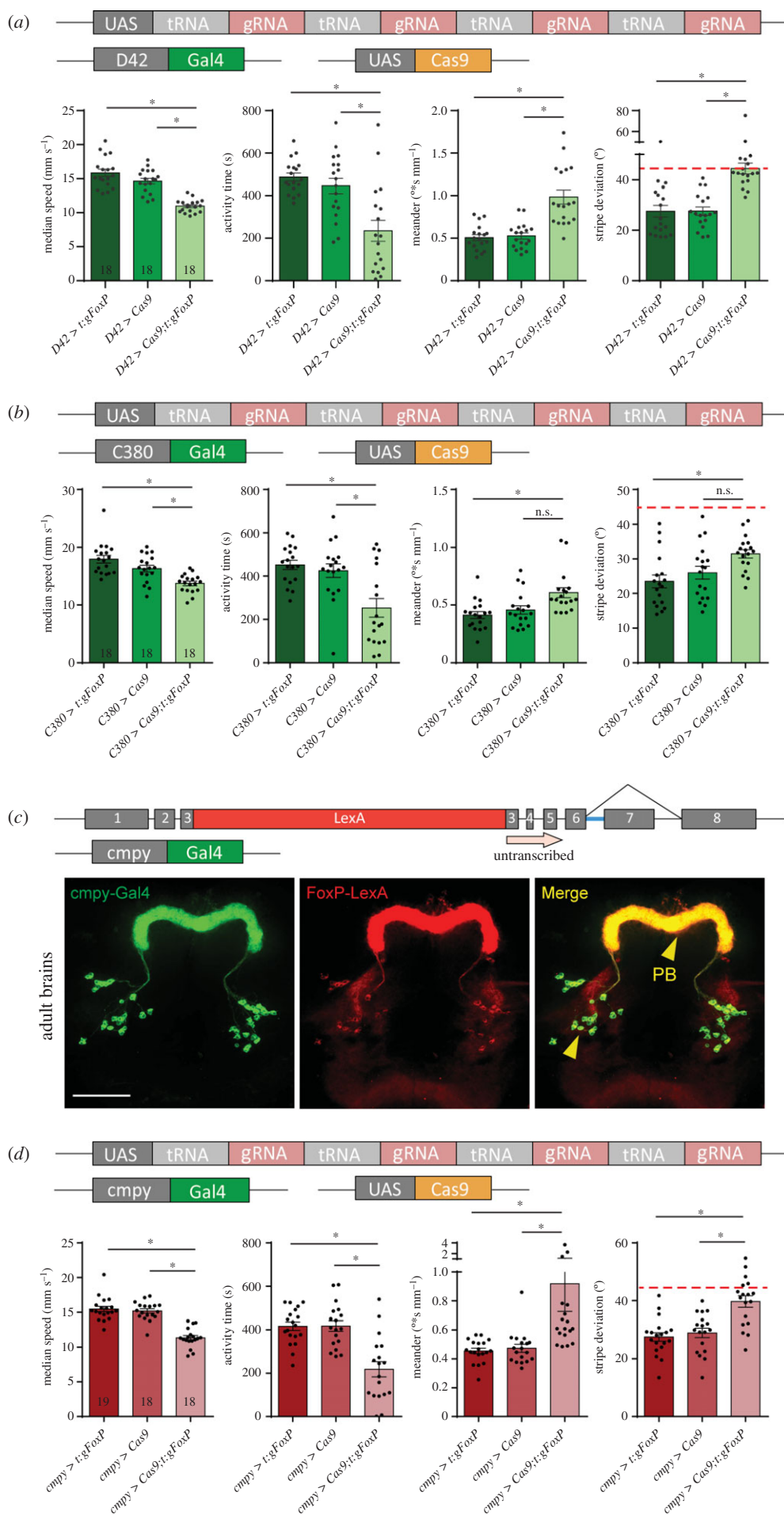
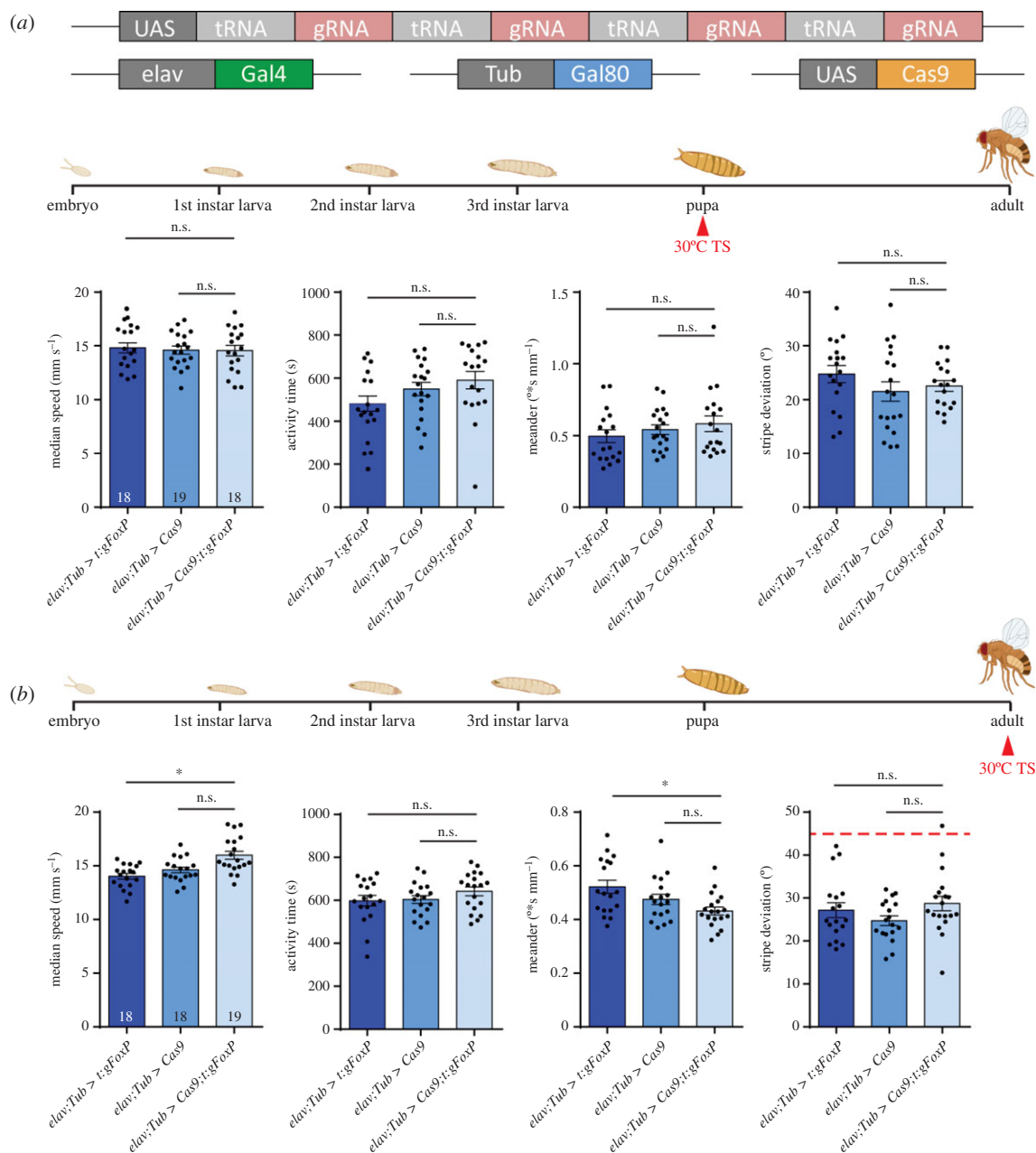


Figure 10. (Caption overleaf.)

**Figure 10.** (*Overleaf.*) *FoxP* is required in both motor neurons and protocerebral bridge for normal walking behaviour in Buridan's paradigm. (*a,b*) Both motor neuron-specific driver lines (*a*) *D42-Gal4* (non-parametric tests for speed, activity time and meander) and (*b*) *C380-Gal4* show similar reductions in walking speed and activity time, but the spatial parameters fail to reach statistical significance despite trending in the same direction as in *D42*. (*c*) The *cmpy-Gal4* driver stains an overlapping set of protocerebral bridge (PB) neurons compared to our *FoxP-LexA* driver line. (*d*) Knocking out the *FoxP* gene in *cmpy-Gal4*-positive neurons leads to similar alterations in walking behaviour in Buridan's paradigm as a complete knock-out, i.e. reduced walking speed, reduced activity time, decreased stripe fixation and increased meander. Non-parametric test for meander. \* $p < 0.005$ .



**Figure 11.** Adult *FoxP* expression is not required for normal locomotor behaviour in Buridan's paradigm. (*a*) Genetic tools used to perform the temporally controlled *FoxP* knock-out. (*b*) Neither temporal (median speed and activity time) nor spatial (meander and stripe deviation) parameters are altered in adult flies in Buridan's paradigm after inducing the *FoxP*-KO in the early pupa. (*c*) Neither temporal nor spatial parameters are changed in adult flies in Buridan's paradigm after inducing the *FoxP*-KO immediately after eclosion. \* $p < 0.005$ .

required for normal locomotion in Buridan's paradigm [41,54,56]. By contrast, without *FoxP* in the protocerebral bridge or motor neurons, flies show similar locomotor impairments as flies with constitutive knock-outs (figure 10). These impairments appear to be due to developmental action of the *FoxP* gene during larval development, as no such effects can be found if the gene is knocked out in all cells in the early pupal or adult stages (figure 11).

## 5.1. *Foxp* expression

### 5.1.1. Neuronal expression of *FoxP* is widespread but not in mushroom bodies

The exact expression pattern of *FoxP* has been under debate for quite some time now. Initial work combined traditional reporter gene expression with immunohistochemistry [21] (table 4).

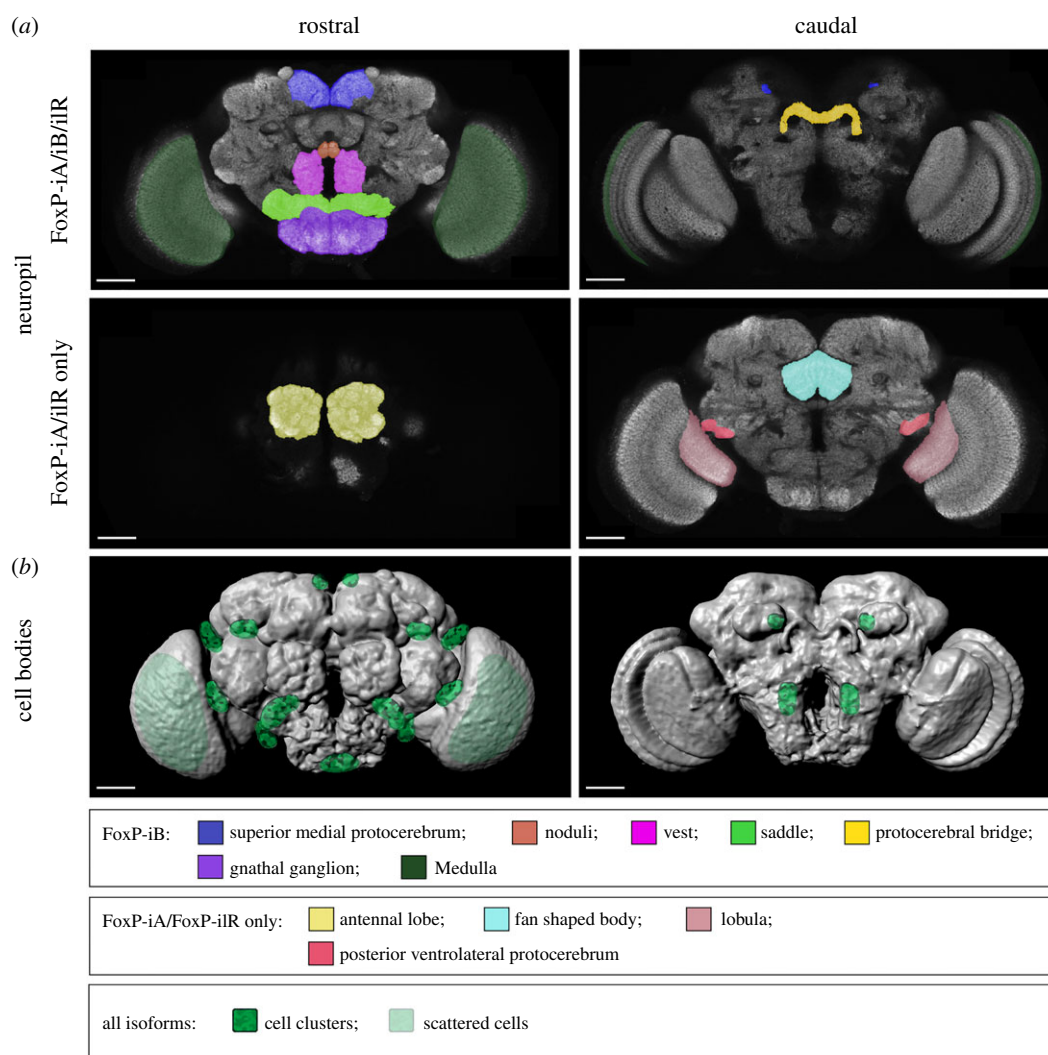


**Figure 12.** *FoxP* expression pattern in the adult *Drosophila* brain. (a) Rostral and caudal sections with neuropil areas marked for *FoxP-iB* expression (above) or for other *FoxP* isoforms excluding *FoxP-iB* (below). (b) Volume rendering of adult neuropil with marked approximate *FoxP*-positive cell body locations in the cortex. Scale bars, 50  $\mu\text{m}$ .

**Table 4.** The four previous reports and the present work describing *FoxP* expression patterns.

publication	method	expression pattern
Lawton <i>et al.</i> [21]	— <i>Gal4</i> (1.5 kb fragment, pGaTB) — antibody	— small number of neurons in various areas of the brain — not mushroom bodies
DasGupta <i>et al.</i> [35]	<i>Gal4</i> (1.4 kb fragment, pBPGUw)	— only mushroom bodies
Schatton & Scharff [62]	<i>Gal4</i> (1.9 kb fragment, pBPGUw)	— mushroom bodies and other areas
Castells-Nobau <i>et al.</i> [20]	— GFP-tag (fosmid) — antibody	— abundant number of neurons in various areas of the brain — not mushroom bodies
present work	— genomic <i>Gal4</i> -tag (CRISPR/Cas9 HDR, pTGEM(0)) — antibody	— abundant number of neurons in various areas of the brain — not mushroom bodies

Lawton and colleagues [21] created a *FoxP-Gal4* line where a 1.5 kb fragment of genomic DNA upstream of the *FoxP* coding region was used to drive Gal4 expression. These authors validated the resulting expression pattern with the staining of a commercial polyclonal antibody against FoxP. We used the same antibody in this work and observed perfect co-expression with our reporter (figure 1c). The Lawton *et al.* description of the *FoxP* expression pattern as a small number of neurons

distributed in various areas of the brain, particularly in the protocerebral bridge, matches our results and those of [20].

Subsequent reports on FoxP expression patterns also used putative FoxP promoter fragments to direct the expression of Gal4 [35,62]. DasGupta and colleagues [35] used a 1.4 kb sequence upstream of the FoxP transcription start site, while Schatton & Scharff [62] used 1.9 kb. Their larger fragment contained the sequences of the two previously used fragments

(table 4). In contrast to [20,21] and our work here, both studies reported expression in overlapping sets of MB Kenyon cells. While DasGupta and colleagues implied that there was no expression outside of the MBs, Schatton and Scharff were not explicit. However, Schatton *et al.* independently reported that they had observed strong expression also outside of the MBs ([63] and A Schatton, C Scharff 2018-2020, personal communication).

The fourth and latest study reporting on *FoxP* expression in *Drosophila* [20] avoided the problematic promoter fragment method and instead tagged *FoxP* within a genomic segment contained in a fosmid [64], intended to ensure expression of GFP-tagged *FoxP* under the control of its own, endogenous regulatory elements. This study was the first to circumvent the potential for artefacts created either by selection of the wrong promoter fragment or by choosing an inappropriate basal promoter with the fragment (see below). However, since they also used insertion of a transgene, their expression pattern, analogous to that of a promoter fragment Gal4 line, may potentially be subject to local effects where the fosmid with the tagged *FoxP* was inserted. Castells-Nobau and colleagues [20] also used the antibody generated by Lawton *et al.* [21] to validate their transgenic expression patterns. The results reported with this technique are similar to those of Lawton *et al.* [21] and our work (summarized in figure 12*b*).

In an attempt to eliminate, the last source of error for determining the expression pattern of *FoxP* in *Drosophila*, we used CRISPR/Cas9 with homology-directed repair to tag *FoxP* *in situ*, avoiding both the potential local insertion effects of the previous approaches and without disrupting the complex regulation that may occur from more distant parts in the genome. For instance, in human cells, there are at least 18 different genomic regions that are in physical contact with the *FOXP2* promoter, some of which act as enhancers [65]. The effects of these regions may be disrupted even if the entire genomic *FoxP* locus were inserted in a different genomic region as in [20]. Interestingly, the first promoter fragment approach [21] and the fosmid approach [20] agree both with our most artefact-avoiding genome editing approach and the immunohistochemistry with an antibody validated by at least three different *FoxP-KO* approaches. This converging evidence from four different methods used in three different laboratories suggests that *FoxP* is expressed in about 1800 neurons in the fly nervous system, of which about 500 are located in the ventral nerve cord. Expression in the brain is widespread with both localized clusters and individual neurons (figure 12*b*) across a variety of neuronal cell types. Notably, the four methods also agree that there is no detectable *FoxP* expression in the adult or larval MBs. By contrast, in honey bees, there is converging evidence of *FoxP* expression in the MBs [62].

## 5.2. Understanding false-positive *FoxP* detection in mushroom bodies

This comparison of our data with the literature prompts the question why two different promoter fragment approaches [35,62] suggested *FoxP* expression in the MBs (confirmed by a ribosome-based approach, see below) when there is no *FoxP* protein detectable there.

A first observation is that Lawton *et al.* used the classic *hsp70*-based pGaTB vector [66] to create their Gal4 line, while both DasGupta *et al.* as well as Schatton and Scharff

used the more modern *Drosophila* synthetic core promoter (DSCP)-based pBPGUw vector [67]. The two vectors differ with regard to their effects on gene expression. In addition to carrying two different basal promoters, the modern pBPGUw sports a 3'UTR that is designed to increase the longevity and stability of the mRNA over the pGaTB vector, which can result in twofold higher Gal4 levels [68].

This observation is complemented by single-cell transcriptome data [69]. *FoxP* RNA can be detected in more than 4100 brain cells, likely overcounting the actual *FoxP* expression more than threefold. For instance, *FoxP* RNA is detected in over 1000 glial cells where none of the published studies has ever detected any *FoxP* expression (see also figure 2).

Taking these two observations together, it becomes plausible that there may be transient, low-level *FoxP* transcription in some MB neurons (and likely thousands of other cells as well), which in wild-type animals rarely leads to any physiologically relevant *FoxP* protein levels in these cells. Only when gene expression is enhanced by combining some arbitrary promoter fragments with genetically engineered constructs designed to maximize Gal4 yield such as the pBPGUw vector, such transient, low-abundance mRNAs may be amplified to a detectable level.

These considerations may also help explain why the ribosome-based method of [34] was able to detect *FoxP* RNA in MB Kenyon cells: the transcript they detected may have been present and occupied by ribosomes, but ribosomal occupancy does not automatically entail translation [70]. It remains unexplained, however, how DasGupta *et al.* failed to detect all those much more strongly expressing and numerous neurons outside of the MBs. All of the above is consistent with other insect species showing *FoxP* expression on the protein level in their MBs [62], as only limited genetic alterations would be needed for such minor changes in gene expression.

The stochasticity of gene expression is a well-known fact [71–79] and known to arise from the transcription machinery [80]. Post-transcriptional gene regulation is similarly well-known [81–86]. It is thus not surprising if we observe that many cells often express transcripts that rarely, if ever, are translated into proteins. The final arbiter of gene expression must therefore remain the protein level, which is why we validated our expression analysis with the appropriate antibody. On this decisive level, *FoxP* has not been detected in the MBs at this point.

## 5.3. Different *FoxP* isoforms are expressed in different neurons

Our genome editing approach allowed us to distinguish differences in the expression patterns of different *FoxP* isoforms. The isoform specifically involved in operant self-learning, *FoxP-iB*, is only expressed in about 65% of all *FoxP*-positive neurons. The remainder express either *FoxP-iA* or *FoxP-iIR* or both. Neurons expressing only non-iB isoforms are localized in the antennal lobes, the fan-shaped body, the lobula and a glomerulus of the posterior ventrolateral protocerebrum (figure 5). Combined with all three isoforms differing in their DNA-binding FH box, the different expression patterns for the different isoforms adds to the emerging picture that the different isoforms may serve very different functions.

## 5.4. *FoxP* and locomotor behaviour

### 5.4.1. *FoxP* is involved in both spatial and temporal parameters of walking

Alterations of *FoxP* family genes universally result in various motor deficits on a broad scale in humans [4,6,7,87] and mice [88–90] for both learned and innate behaviours. Also in flies, manipulations of the *FoxP* locus by mutation or RNA interference have revealed that *FoxP* is involved in flight performance and other, presumably inborn, locomotor behaviours [18,20–22] as well as in motor learning tasks [18].

The locomotor phenotypes described so far largely concerned the temporal aspects of locomotion, such as initiation, speed or duration of locomotor behaviours. Here, using Buridan's paradigm [30,31], we report that manipulations of *FoxP* can also alter spatial aspects of locomotion, such as landmark fixation or the straightness of trajectories. Our results further exemplify the old insight that coarse assaults on gene function such as constitutive knock-outs of entire genes or isoforms very rarely yield useful, specific phenotypes [91]. Rather, it is often the most delicate of manipulations that reveal the involvement of a particular gene in a specific behaviour. This fact is likely most often due to the pleiotropy of genes, often paired with differential dominance which renders coarse neurogenetic approaches useless in most instances, as so many different behaviours are affected that the specific contribution of a gene to a behavioural phenotype becomes impossible to dissect.

In the case of *FoxP*, it was already known, for instance, that the different isoforms affect flight performance to differing degrees [18] and that a variety of different *FoxP* manipulations affected general locomotor activity [20–22]. Here we show that a complete knock-out of either *FoxP-iB* or all isoforms affected both spatial and temporal parameters of locomotion, but the insertion mutation *FoxP*<sup>3955</sup> did not alter stripe fixation (figures 6 and 7). Remarkably, despite the ubiquitous and substantial locomotor impairments after nearly any kind of *FoxP* manipulation be it genomic or via RNAi reported in the published literature, DasGupta *et al.* [35], failed to detect the locomotor defects of these flies.

While some of our manipulations did not affect locomotion significantly (e.g. knock-out in MBs or DCNs, figure 9, see below for discussion), most of them affected both spatial and temporal locomotion parameters (e.g. Figures 6,7,9), despite these parameters commonly not co-varying [92]. Thus, while one would expect these behaviours to be biologically separable, our manipulations did not succeed in this separation.

### 5.4.2. Locomotion does not require *FoxP* expression in all *FoxP* neurons

Taken together, the results available to-date reveal *FoxP* to be a highly pleiotropic gene with phenotypes that span both temporal and spatial domains of locomotion in several behavioural modalities, lifespan, motor learning, social behaviour and habituation. It is straightforward to conclude that only precise, cell-type-specific *FoxP* manipulations of specific isoforms will be capable of elucidating the function this gene serves in each phenotype. With RNAi generally yielding varying levels of knock-down and, specifically, with currently available *FoxP* RNAi lines showing only little, if any, detectable knock-down with RT-qPCR (data deposited at doi:10.6084/m9.

figshare.12607667 and Annette Schenck, personal communication), CRISPR/Cas9-mediated genome editing lends itself as the method of choice for this task. Practical considerations when designing multi-target gRNAs for *FoxP* prompted us to begin testing the CRISPR/Cas9 system as an alternative to RNAi with an isoform-unspecific approach first, keeping the isoform-specific approach for a time when we have collected more experience in this technique. In a first proof-of-principle, we used CRISPR/Cas9 to remove *FoxP* from MB Kenyon cells, DCNs, motor neurons and the protocerebral bridge.

MBs have been shown to affect both spatial and temporal aspects of locomotion [e.g. 51–60] and Castells-Nobau *et al.* [20] reported a subtle structural phenotype in a subset of MB Kenyon cells that did not express *FoxP*. As detailed above, two groups have reported *FoxP* expression in the MBs and it appears that some transcript can be found in MB Kenyon cells. With a substantial walking defect both in *FoxP*<sup>3955</sup> mutant flies (which primarily affects *FoxP-iB* expression [18]) and in flies without any *FoxP* (figure 7), together with the MBs being critical for normal walking behaviour, the MBs were a straightforward candidate for a cell-type-specific *FoxP-KO*. However, flies without *FoxP* in the MBs walk perfectly normally (figure 9c). There are two possible reasons for this lack of an effect of our manipulation: either *FoxP* protein is not present in MBs or it is not important in MBs for walking. While at this point we are not able to decide between these two options, our expression data concurring with those from previous studies [20,21] suggest the former explanation may be the more likely one (see also above). Remarkably, a publication that did report *FoxP* expression in the MBs [35] did not detect the walking deficits in *FoxP*<sup>3955</sup> mutant flies despite testing for such effects. Motor aberrations as those described here and in other *FoxP* manipulations [20–22,36] constitute a potential alternative to the decision-making impairments ascribed to these flies in DasGupta *et al.* [35].

DCNs were recently shown to be involved in the spatial component (landmark fixation) of walking in Buridan's paradigm [41], but removing *FoxP* from DCNs showed no effect (figure 9b), despite abundant *FoxP* expression in DCNs (figure 9a). It is possible that a potential effect in stripe fixation may have been masked by already somewhat low fixation in both control strains. On the other hand, even at such control fixation levels, significant increases in stripe deviation can be obtained (e.g. Figure 10a). Before this is resolved, one explanation is that *FoxP* is not required in these neurons for landmark fixation in Buridan's paradigm, while the neurons themselves are required.

Motor neurons are involved in all aspects of behaviour and have been shown to be important for operant self-learning [61]. With abundant expression of *FoxP* in motor neurons (figure 3a), we considered these neurons a prime candidate for a clear *FoxP-cKO* phenotype. Indeed, removing *FoxP* specifically from motor neurons only, mimicked the effects of removing the gene constitutively from all cells (figure 10a,b). It is noteworthy that this manipulation alone was sufficient to affect both temporal and spatial parameters, albeit only one of the two driver lines showed clear-cut results (D42). One would not necessarily expect motor neurons to affect purportedly 'higher-order' functions such as landmark fixation. It is possible that the higher tortuosity in the trajectories of the flies where D42 was used to drive our UAS-gRNA construct is largely responsible for the greater angular deviation from the landmarks in these flies and that this tortuosity, in turn is caused by the missing

FoxP in motor neurons. Alternatively, D42 is also driving in non-motor neurons where *FoxP* is responsible for landmark fixation. The driver line C380 showed similar trends, albeit not quite statistically significant at our alpha value of 0.5%, suggesting that potentially the increased meander parameter may be caused by motor neurons lacking *FoxP*.

The protocerebral bridge is not only the arguably most conspicuous *FoxP*-positive neuropil, it has also been reported to be involved in temporal aspects of walking [93–95]. Moreover, the protocerebral bridge provides input to other components of the central complex involved in angular orientation [22,96–98]. Similar to the results in motor neurons, removing *FoxP* from a small group of brain neurons innervating the protocerebral bridge, phenocopies constitutive *FoxP* mutants.

Taken together, the motor neuron and protocerebral bridge results suggest that both sets of neurons serve their locomotor function in sequence. At this point, it is unclear which set of neurons precedes the other in this sequence.

#### 5.4.3. *FoxP* is only required during larval development to ensure normal locomotion

There is ample evidence that the *FoxP* family of transcription factors acts during development in a variety of tissues [9,99,100]. What is less well known is if adult *FoxP* expression serves any specific function. A recent study in transgenic mice in operant conditioning and motor learning tasks showed postnatal knock-out of FOXP2 in cerebellar and striatal neurons affected leverpressing and cerebellar knock-out also affected motor-learning [90]. At least for these tasks in

mammals, a *FoxP* family member does serve a postnatal function that is independent of brain development (brain morphology was unaltered in these experiments). Also in birds, evidence has been accumulating that adult *FoxP* expression serves a song plasticity function [101–106]. Our temporally controlled experiments (figures 8 and 11) suggest that at least locomotion in Buridan's paradigm can function normally in the absence of *FoxP* expression in the adult, as long as *FoxP* expression remains unaltered during larval development. Future research on the role of *FoxP* in locomotion and landmark fixation hence needs to focus on the larval development before pupation.

**Data accessibility.** All original raw data are deposited with figshare (<http://figshare.com>), references in the text. All raw data are publicly accessible with an Attribution 4.0 International (CC BY 4.0) license. Data sources for specific figures are referenced in the text. A compressed file with all the data is also available [33].

**Authors' contributions.** Conceived and designed the experiments: O.P., M.R. and B.B. Performed the experiments: O.P. Analysed the data: O.P., M.R. and B.B. Contributed reagents/materials/analysis tools: M.R. and B.B. Wrote the paper: O.P. and B.B. Initiated the project: B.B. Critically revised the manuscript: O.P., M.R. and B.B. The authors declare no existing conflicts of interest.

**Competing interests.** We declare we have no competing interests.

**Funding.** This project was funded by the DFG (Deutsche Forschungsgemeinschaft, grant no. BR 1892/17-1).

**Acknowledgements.** Technical assistance was provided by Klara Krmpotić (Buridan experiments with *FoxP-iB-Gal4*) and Marcela Loza. We are indebted to David Deitcher for sharing his FoxP antibody with us. We are grateful to three anonymous reviewers for their insightful suggestions, which significantly increased the quality of the manuscript.

## References

- Hannenhalli S, Kaestner KH. 2009 The evolution of Fox genes and their role in development and disease. *Nat. Rev. Genet.* **10**, 233–240. (doi:10.1038/nrg2523)
- Santos ME, Athanasiadis A, Leitão AB, DuPasquier L, Sucena E. 2011 Alternative splicing and gene duplication in the evolution of the FoxP gene subfamily. *Mol. Biol. Evol.* **28**, 237–247. (doi:10.1093/molbev/msq182)
- Golson ML, Kaestner KH. 2016 Fox transcription factors: from development to disease. *Development* **143**, 4558–4570. (doi:10.1242/dev.112672)
- den Hoed J, Fisher SE. 2020 Genetic pathways involved in human speech disorders. *Curr. Opin. Genet. Dev.* **65**, 103–111. (doi:10.1016/j.gde.2020.05.012)
- Lai CS, Fisher SE, Hurst JA, Vargha-Khadem F, Monaco AP. 2001 A forkhead-domain gene is mutated in a severe speech and language disorder. *Nature* **413**, 519–523. (doi:10.1038/35097076)
- Reuter MS *et al.* 2017 FOXP2 variants in 14 individuals with developmental speech and language disorders broaden the mutational and clinical spectrum. *J. Med. Genet.* **54**, 64–72. (doi:10.1136/jmedgenet-2016-104094)
- Carr CW, Moreno-De-Luca D, Parker C, Zimmerman HH, Ledbetter N, Martin CL, Dobyns WB, Abdul-Rahman OA. 2010 Chiari I malformation, delayed gross motor skills, severe speech delay, and epileptiform discharges in a child with FOXP1 haploinsufficiency. *Eur. J. Hum. Genet.* **18**, 1216–1220. (doi:10.1038/ejhg.2010.96)
- Horn D *et al.* 2010 Identification of FOXP1 deletions in three unrelated patients with mental retardation and significant speech and language deficits. *Hum. Mutat.* **31**, E1851–E1860. (doi:10.1002/humu.21362)
- Co M, Anderson AG, Konopka G. 2020 FOXP transcription factors in vertebrate brain development, function, and disorders. *Wiley Interdiscip. Rev. Dev. Biol.* **9**, e375. (doi:10.1002/wdev.375)
- Hagoort P. 2019 *Human language: from genes and brains to behavior*. New York, NY: MIT Press.
- Schatton A, Scharff C. 2016 Next stop: language. The 'FOXP2' gene's journey through time. *Métode* **0**. (doi:10.7203/metode.7.7248)
- Bolhuis JJ. 2011 Twitter evolution: parallel brain mechanisms of auditory–vocal learning in songbirds and humans. *Neurosci. Res.* **71**, e19. (doi:10.1016/j.neures.2011.07.080)
- Morgan A, Fisher SE, Scheffer I, Hildebrand M. 2016 Related speech and language disorders. In *Genereviews* (eds MP Adam, HH Ardinger, RA Pagon, SE Wallace, LH Bean, K Stephens, A Amemiya), Seattle, WA: University of Washington.
- Haesler S, Rochefort C, Georgi B, Licznarski P, Osten P, Scharff C. 2007 Incomplete and inaccurate vocal imitation after knockdown of FoxP2 in songbird basal ganglia nucleus Area X. *PLoS Biol.* **5**, e321. (doi:10.1371/journal.pbio.0050321)
- Naour P. 2009 *E.O. Wilson and B.F. Skinner*. New York, NY: Springer.
- Marler P. 1991 Song-learning behavior: the interface with neuroethology. *Trends Neurosci.* **14**, 199–206. (doi:10.1016/0166-2236(91)90106-5)
- Fee MS. 2014 The role of efference copy in striatal learning. *Curr. Opin. Neurobiol.* **25**, 194–200. (doi:10.1016/j.conb.2014.01.012)
- Mendoza E, Colomb J, Rybak J, Pflüger H-J, Zars T, Scharff C, Brems B. 2014 *Drosophila* FoxP mutants are deficient in operant self-learning. *PLoS ONE* **9**, e100648. (doi:10.1371/journal.pone.0100648)
- Weigel D, Jürgens G, Küttner F, Seifert E, Jäckle H. 1989 The homeotic gene fork head encodes a nuclear protein and is expressed in the terminal regions of the *Drosophila* embryo. *Cell* **57**, 645–658. (doi:10.1016/0092-8674(89)90133-5)
- Castells-Nobau A *et al.* 2019 Conserved regulation of neurodevelopmental processes and behavior by FoxP in *Drosophila*. *PLoS ONE* **14**, e0211652. (doi:10.1371/journal.pone.0211652)
- Lawton KJ, Wassmer TL, Deitcher DL. 2014 Conserved role of *Drosophila melanogaster* FoxP in

- motor coordination and courtship song. *Behav. Brain Res.* **268**, 213–221. (doi:10.1016/j.bbr.2014.04.009)
22. Kottler B, Faville R, Bridi JC, Hirth F. 2019 Inverse control of turning behavior by dopamine D1 receptor signaling in columnar and ring neurons of the central complex in *Drosophila*. *Curr. Biol.* **29**, 567–577. (doi:10.1016/j.cub.2019.01.017)
  23. McGuire SE, Le PT, Osborn AJ, Matsumoto K, Davis RL. 2003 Spatiotemporal rescue of memory dysfunction in *Drosophila*. *Science* **302**, 1765–1768. (doi:10.1126/science.1089035)
  24. McGuire SE, Mao Z, Davis RL. 2004 Spatiotemporal gene expression targeting with the TARGET and gene-switch systems in *Drosophila*. *Sci. STKE* **2004**, 16.
  25. Gratz SJ, Ukken FP, Rubinstein CD, Thiede G, Donohue LK, Cummings AM, O'Connor-Giles KM. 2014 Highly specific and efficient CRISPR/Cas9-catalyzed homology-directed repair in *Drosophila*. *Genetics* **196**, 961–971. (doi:10.1534/genetics.113.160713)
  26. Port F, Bullock SL. 2016 Augmenting CRISPR applications in *Drosophila* with tRNA-flanked sgRNAs. *Nat. Methods* **13**, 852–854. (doi:10.1038/nmeth.3972)
  27. Diao F *et al.* 2015 Plug-and-play genetic access to *Drosophila* cell types using exchangeable exon cassettes. *Cell Rep.* **10**, 1410–1421. (doi:10.1016/j.celrep.2015.01.059)
  28. Shan Q *et al.* 2013 Targeted genome modification of crop plants using a CRISPR-Cas system. *Nat. Biotechnol.* **31**, 686–688. (doi:10.1038/nbt.2650)
  29. Rueden CT, Schindelin J, Hiner MC, DeZonia BE, Walter AE, Arena ET, Eliceiri KW. 2017 ImageJ2: ImageJ for the next generation of scientific image data. *BMC Bioinformatics* **18**, 529. (doi:10.1186/s12859-017-1934-z)
  30. Götz KG. 1980 Visual guidance in *Drosophila*. *Basic Life Sci.* **16**, 391–407. (doi:10.1007/978-1-4684-7968-3\_28)
  31. Colomb J, Reiter L, Blaszkiewicz J, Wessnitzer J, Brembs B. 2012 Open source tracking and analysis of adult *Drosophila* locomotion in Buridan's paradigm with and without visual targets. *PLoS ONE* **7**, e42247. (doi:10.1371/journal.pone.0042247)
  32. Benjamin DJ *et al.* 2018 Redefine statistical significance. *Nat. Hum. Behav.* **2**, 6–10. (doi:10.1038/s41562-017-0189-z)
  33. Palazzo O, Brembs B. 2020 FoxP expression analysis and role in locomotion. Identification of FoxP circuits involved in locomotion and object fixation in *Drosophila*. *Figshare*. (doi:10.6084/m9.figshare.12656177)
  34. Groschner LN, Chan Wah Hak L, Bogacz R, DasGupta S, Miesenböck G. 2018 Dendritic integration of sensory evidence in perceptual decision-making. *Cell* **173**, 894–905. (doi:10.1016/j.cell.2018.03.075)
  35. DasGupta S, Ferreira CH, Miesenböck G. 2014 FoxP influences the speed and accuracy of a perceptual decision in *Drosophila*. *Science* **344**, 901–904. (doi:10.1126/science.1252114)
  36. Lawton K. 2014 Conserved role of *Drosophila melanogaster* Foxp. In *Motor coordination And courtship song*. PhD, Cornell University. See <https://ecommons.cornell.edu/handle/1813/36103>.
  37. Schatton A, Agoro J, Mardink J, Leboulle G, Scharff C. 2018 Identification of the neurotransmitter profile of AmFoxP expressing neurons in the honeybee brain using double-label *in situ* hybridization. *BMC Neurosci.* **19**, 69. (doi:10.1186/s12868-018-0469-1)
  38. Pollock JA, Ellisman MH, Benzer S. 1990 Subcellular localization of transcripts in *Drosophila* photoreceptor neurons: chaoptic mutants have an aberrant distribution. *Genes Dev.* **4**, 806–821. (doi:10.1101/gad.4.5.806)
  39. Szüts D, Bienz M. 2000 LexA chimeras reveal the function of *Drosophila* Fos as a context-dependent transcriptional activator. *Proc. Natl Acad. Sci. USA* **97**, 5351–5356. (doi:10.1073/pnas.97.10.5351)
  40. Xie K, Minkenberg B, Yang Y. 2015 Boosting CRISPR/Cas9 multiplex editing capability with the endogenous tRNA-processing system. *Proc. Natl Acad. Sci. USA* **112**, 3570–3575. (doi:10.1073/pnas.1420294112)
  41. Linneweber GA *et al.* 2020 A neurodevelopmental origin of behavioral individuality in the *Drosophila* visual system. *Science* **367**, 1112–1119. (doi:10.1126/science.aaw7182)
  42. Hassan BA, Bermingham NA, He Y, Sun Y, Jan YN, Zoghbi HY, Bellen HJ. 2000 Atonal regulates neurite arborization but does not act as a proneural gene in the *Drosophila* brain. *Neuron* **25**, 549–561. (doi:10.1016/S0896-6273(00)81059-4)
  43. Warth Pérez Arias CC, Frosch P, Fiala A, Riemensperger TD. 2020 Stochastic and arbitrarily generated input patterns to the mushroom bodies can serve as conditioned stimuli in. *Front. Physiol.* **11**, 53. (doi:10.3389/fphys.2020.00053)
  44. Lyutova R *et al.* 2019 Reward signaling in a recurrent circuit of dopaminergic neurons and peptidergic Kenyon cells. *Nat. Commun.* **10**, 3097. (doi:10.1038/s41467-019-11092-1)
  45. König C, Khalili A, Niewalda T, Gao S, Gerber B. 2019 An optogenetic analogue of second-order reinforcement in *Drosophila*. *Biol. Lett.* **15**, 20190084. (doi:10.1098/rsbl.2019.0084)
  46. Thum AS, Gerber B. 2019 Connectomics and function of a memory network: the mushroom body of larval *Drosophila*. *Curr. Opin. Neurobiol.* **54**, 146–154. (doi:10.1016/j.conb.2018.10.007)
  47. Widmer YF, Fritsch C, Jungo MM, Almeida S, Egger B, Sprecher SG. 2018 Multiple neurons encode CrebB dependent appetitive long-term memory in the mushroom body circuit. *Elife* **7**, e39196. (doi:10.7554/eLife.39196)
  48. Felsenberg J *et al.* 2018 Integration of parallel opposing memories underlies memory extinction. *Cell* **175**, 709–722. (doi:10.1016/j.cell.2018.08.021)
  49. Dolan M-J *et al.* 2018 Communication from learned to innate olfactory processing centers is required for memory retrieval in *Drosophila*. *Neuron* **100**, 651–668. (doi:10.1016/j.neuron.2018.08.037)
  50. Turrel O, Goguel V, Preat T. 2018 Amnesiac is required in the adult mushroom body for memory formation. *J. Neurosci.* **38**, 9202–9214. (doi:10.1523/JNEUROSCI.0876-18.2018)
  51. Martin JR, Ernst R, Heisenberg M. 1998 Mushroom bodies suppress locomotor activity in *Drosophila melanogaster*. *Learn. Mem.* **5**, 179–191.
  52. Helfrich-Förster C, Wulf J, de Belle JS. 2002 Mushroom body influence on locomotor activity and circadian rhythms in *Drosophila melanogaster*. *J. Neurogenet.* **16**, 73–109. (doi:10.1080/01677060213158)
  53. Besson M, Martin J-R. 2005 Centrophobism/thigmotaxis, a new role for the mushroom bodies in *Drosophila*. *J. Neurobiol.* **62**, 386–396. (doi:10.1002/neu.20111)
  54. Serway CN, Kaufman RR, Strauss R, de Belle JS. 2009 Mushroom bodies enhance initial motor activity in *Drosophila*. *J. Neurogenet.* **23**, 173–184. (doi:10.1080/01677060802572895)
  55. Lebreton S, Martin J-R. 2009 Mutations affecting the cAMP transduction pathway disrupt the centrophobism behavior. *J. Neurogenet.* **23**, 225–234. (doi:10.1080/01677060802509160)
  56. Xiong Y, Lv H, Gong Z, Liu L. 2010 Fixation and locomotor activity are impaired by inducing tetanus toxin expression in adult *Drosophila* brain. *Fly* **4**, 194–203. (doi:10.4161/fly.12668)
  57. Mabuchi I, Shimada N, Sato S, Ienaga K, Inami S, Sakai T. 2016 Mushroom body signaling is required for locomotor activity rhythms in *Drosophila*. *Neurosci. Res.* **111**, 25–33. (doi:10.1016/j.neures.2016.04.005)
  58. Lark A, Kitamoto T, Martin J-R. 2017 Modulation of neuronal activity in the *Drosophila* mushroom body by DopEcR, a unique dual receptor for ecdysone and dopamine. *Biochim. Biophys. Acta Mol. Cell Res.* **1864**, 1578–1588. (doi:10.1016/j.bbamcr.2017.05.015)
  59. Sun J, Xu AQ, Giraud J, Poppinga H, Riemensperger T, Fiala A, Birman S. 2018 Neural control of startle-induced locomotion by the mushroom bodies and associated neurons in. *Front. Syst. Neurosci.* **12**, 6. (doi:10.3389/fnsys.2018.00006)
  60. Manjila SB, Kuruvilla M, Ferveur J-F, Sane SP, Hasan G. 2019 Extended flight bouts require disinhibition from GABAergic mushroom body neurons. *Curr. Biol.* **29**, 283–293. (doi:10.1016/j.cub.2018.11.070)
  61. Colomb J, Brembs B. 2016 PKC in motor neurons underlies self-learning, a form of motor learning in *Drosophila*. *PeerJ* **4**, e1971. (doi:10.7717/peerj.1971)
  62. Schatton A, Scharff C. 2017 FoxP expression identifies a Kenyon cell subtype in the honeybee mushroom bodies linking them to fruit fly  $\alpha\beta c$  neurons. *Eur. J. Neurosci.* **46**, 2534–2541. (doi:10.1111/ejn.13713)
  63. Schatton A. 2018 FoxP in bees and flies—conservation at different levels?: an analysis of sequence, neurons, circuits and behavior. PhD thesis, Freie Universität Berlin.
  64. Kim UJ, Shizuya H, de Jong PJ, Birren B, Simon MI. 1992 Stable propagation of cosmid sized human DNA inserts in an F factor based vector. *Nucleic Acids Res.* **20**, 1083–1085. (doi:10.1093/nar/20.5.1083)

65. Becker M, Devanna P, Fisher SE, Vernes SC. 2018 Mapping of human FOXP2 enhancers reveals complex regulation. *Front. Mol. Neurosci.* **11**, 47. (doi:10.3389/fnmol.2018.00047)
66. Brand AH, Perrimon N. 1993 Targeted gene expression as a means of altering cell fates and generating dominant phenotypes. *Development* **118**, 401–415.
67. Pfeiffer BD *et al.* 2008 Tools for neuroanatomy and neurogenetics in *Drosophila*. *Proc. Natl Acad. Sci. USA* **105**, 9715–9720. (doi:10.1073/pnas.0803697105)
68. Pfeiffer BD, Ngo T-TB, Hibbard KL, Murphy C, Jenett A, Truman JW, Rubin GM. 2010 Refinement of tools for targeted gene expression in *Drosophila*. *Genetics* **186**, 735–755. (doi:10.1534/genetics.110.119917)
69. Davie K *et al.* 2018 A single-cell transcriptome atlas of the aging *Drosophila* brain. *Cell* **174**, 982–998. (doi:10.1016/j.cell.2018.05.057)
70. Guttman M, Russell P, Ingolia NT, Weissman JS, Lander ES. 2013 Ribosome profiling provides evidence that large noncoding RNAs do not encode proteins. *Cell* **154**, 240–251. (doi:10.1016/j.cell.2013.06.009)
71. Elowitz MB, Levine AJ, Siggia ED, Swain PS. 2002 Stochastic gene expression in a single cell. *Science* **297**, 1183–1186. (doi:10.1126/science.1070919)
72. Raser JM, O'Shea EK. 2004 Control of stochasticity in eukaryotic gene expression. *Science* **304**, 1811–1814. (doi:10.1126/science.1098641)
73. Swain PS, Elowitz MB, Siggia ED. 2002 Intrinsic and extrinsic contributions to stochasticity in gene expression. *Proc. Natl Acad. Sci. USA* **99**, 12 795–12 800. (doi:10.1073/pnas.162041399)
74. Volfson D, Marciniak J, Blake WJ, Ostroff N, Tsimring LS, Hasty J. 2006 Origins of extrinsic variability in eukaryotic gene expression. *Nature* **439**, 861–864. (doi:10.1038/nature04281)
75. Neildez-Nguyen TMA *et al.* 2008 Epigenetic gene expression noise and phenotypic diversification of clonal cell populations. *Differentiation* **76**, 33–40. (doi:10.1111/j.1432-0436.2007.00219.x)
76. Thattai M, van Oudenaarden A. 2001 Intrinsic noise in gene regulatory networks. *Proc. Natl Acad. Sci. USA* **98**, 8614–8619. (doi:10.1073/pnas.151588598)
77. Chalancon G, Ravarani CNJ, Balaji S, Martinez-Arias A, Aravind L, Jothi R, Babu MM. 2012 Interplay between gene expression noise and regulatory network architecture. *Trends Genet.* **28**, 221–232. (doi:10.1016/j.tig.2012.01.006)
78. Munsy B, Neuert G, van Oudenaarden A. 2012 Using gene expression noise to understand gene regulation. *Science* **336**, 183–187. (doi:10.1126/science.1216379)
79. Dunlop MJ, Cox 3rd RS, Levine JH, Murray RM, Elowitz MB. 2008 Regulatory activity revealed by dynamic correlations in gene expression noise. *Nat. Genet.* **40**, 1493–1498. (doi:10.1038/ng.281)
80. Quarton T, Kang T, Papakis V, Nguyen K, Nowak C, Li Y, Bleris L. 2020 Uncoupling gene expression noise along the central dogma using genome engineered human cell lines. *Nucleic Acids Res.* **48**, 9406–9413. (doi:10.1093/nar/gkaa668)
81. Cibois M, Gautier-Courteille C, Legagneux V, Paillard L. 2010 Post-transcriptional controls — adding a new layer of regulation to clock gene expression. *Trends Cell Biol.* **20**, 533–541. (doi:10.1016/j.tcb.2010.06.004)
82. Halbeisen RE, Galgano A, Scherrer T, Gerber AP. 2008 Post-transcriptional gene regulation: from genome-wide studies to principles. *Cell. Mol. Life Sci.* **65**, 798–813. (doi:10.1007/s00018-007-7447-6)
83. Engels BM, Hutvagner G. 2006 Principles and effects of microRNA-mediated post-transcriptional gene regulation. *Oncogene* **25**, 6163–6169. (doi:10.1038/sj.onc.1209909)
84. Klausner RD, Harford JB. 1989 Cis-trans models for post-transcriptional gene regulation. *Science* **246**, 870–872. (doi:10.1126/science.2683086)
85. Glisovic T, Bachorik JL, Yong J, Dreyfuss G. 2008 RNA-binding proteins and post-transcriptional gene regulation. *FEBS Lett.* **582**, 1977–1986. (doi:10.1016/j.febslet.2008.03.004)
86. Zhao BS, Roundtree IA, He C. 2017 Post-transcriptional gene regulation by mRNA modifications. *Nat. Rev. Mol. Cell Biol.* **18**, 31–42. (doi:10.1038/nrm.2016.132)
87. Palumbo O, D'Aguma L, Minenna AF, Palumbo P, Stallone R, Palladino T, Zelante L, Carella M. 2013 3p14.1 De novo microdeletion involving the FOXP1 gene in an adult patient with autism, severe speech delay and deficit of motor coordination. *Gene* **516**, 107–113. (doi:10.1016/j.gene.2012.12.073)
88. Chabout J, Sarkar A, Patel SR, Radden T, Dunson DB, Fisher SE, Jarvis ED. 2016 A Foxp2 mutation implicated in human speech deficits alters sequencing of ultrasonic vocalizations in adult male mice. *Front. Behav. Neurosci.* **10**, 197. (doi:10.3389/fnbeh.2016.00197)
89. Usui N, Co M, Harper M, Rieger MA, Dougherty JD, Konopka G. 2017 Sumoylation of FOXP2 regulates motor function and vocal communication through purkinje cell development. *Biol. Psychiatry* **81**, 220–230. (doi:10.1016/j.biopsych.2016.02.008)
90. French CA, Vinuela Veloz MF, Zhou K, Peter S, Fisher SE, Costa RM, De Zeeuw CI. 2019 Differential effects of Foxp2 disruption in distinct motor circuits. *Mol. Psychiatry* **24**, 447–462. (doi:10.1038/s41380-018-0199-x)
91. Pflugfelder GO. 1998 Genetic lesions in *Drosophila* behavioural mutants. *Behav. Brain Res.* **95**, 3–15. (doi:10.1016/S0166-4328(97)00204-0)
92. Colomb J, Brembs B. 2014 Sub-strains of *Drosophila* Canton-S differ markedly in their locomotor behavior. *F1000Research.* **3**, 176. (doi:10.12688/f1000research.4263.1)
93. Strauss R, Hanesch U, Kinkelin M, Wolf R, Heisenberg M. 1992 No-bridge of *Drosophila melanogaster*: portrait of a structural brain mutant of the central complex. *J. Neurogenet.* **8**, 125–155. (doi:10.3109/01677069209083444)
94. Poeck B, Triphan T, Neuser K, Strauss R. 2008 Locomotor control by the central complex in *Drosophila*—an analysis of the *tay bridge* mutant. *Dev. Neurobiol.* **68**, 1046–1058. (doi:10.1002/dneu.20643)
95. Martin JR, Raabe T, Heisenberg M. 1999 Central complex substructures are required for the maintenance of locomotor activity in *Drosophila melanogaster*. *J. Comp. Physiol. A* **185**, 277–288. (doi:10.1007/s003590050387)
96. Su T-S, Lee W-J, Huang Y-C, Wang C-T, Lo C-C. 2017 Coupled symmetric and asymmetric circuits underlying spatial orientation in fruit flies. *Nat. Commun.* **8**, 139. (doi:10.1038/s41467-017-00191-6)
97. Kim SS, Hermundstad AM, Romani S, Abbott LF, Jayaraman V. 2019 Generation of stable heading representations in diverse visual scenes. *Nature* **576**, 126–131. (doi:10.1038/s41586-019-1767-1)
98. Seelig JD, Jayaraman V. 2015 Neural dynamics for landmark orientation and angular path integration. *Nature* **521**, 186–191. (doi:10.1038/nature14446)
99. Lu MM, Li S, Yang H, Morrissey EE. 2002 Foxp4: a novel member of the Foxp subfamily of winged-helix genes co-expressed with Foxp1 and Foxp2 in pulmonary and gut tissues. *Mech. Dev.* **119**(Suppl. 1), S197–S202. (doi:10.1016/S0925-4773(03)00116-3)
100. Shu W, Lu MM, Zhang Y, Tucker PW, Zhou D, Morrissey EE. 2007 Foxp2 and Foxp1 cooperatively regulate lung and esophagus development. *Development* **134**, 1991–2000. (doi:10.1242/dev.02846)
101. Day NF, Hobbs TG, Heston JB, White SA. 2019 Beyond critical period learning: striatal FoxP2 affects the active maintenance of learned vocalizations in adulthood. *eNeuro* **6**, ENEURO.0071-19.2019. (doi:10.1523/ENEURO.0071-19.2019)
102. Teramitsu I, White SA. 2006 FoxP2 regulation during undirected singing in adult songbirds. *J. Neurosci.* **26**, 7390–7394. (doi:10.1523/JNEUROSCI.1662-06.2006)
103. Miller JE, Spiteri E, Condro MC, Dosumu-Johnson RT, Geschwind DH, White SA. 2008 Birdsong decreases protein levels of FoxP2, a molecule required for human speech. *J. Neurophysiol.* **100**, 2015–2025. (doi:10.1152/jn.90415.2008)
104. Chen Q, Heston JB, Burkett ZD, White SA. 2013 Expression analysis of the speech-related genes FoxP1 and FoxP2 and their relation to singing behavior in two songbird species. *J. Exp. Biol.* **216**, 3682–3692. (doi:10.1242/jeb.085886)
105. Shi Z, Luo G, Fu L, Fang Z, Wang X, Li X. 2013 miR-9 and miR-140-5p target FoxP2 and are regulated as a function of the social context of singing behavior in zebra finches. *J. Neurosci.* **33**, 16 510–16 521. (doi:10.1523/JNEUROSCI.0838-13.2013)
106. Thompson CK, Schwabe F, Schoof A, Mendoza E, Gampe J, Rochefort C, Scharff C. 2013 Young and intense: FoxP2 immunoreactivity in Area X varies with age, song stereotypy, and singing in male zebra finches. *Front. Neural Circuits* **7**, 24. (doi:10.3389/fncir.2013.00024)